

Academic Communication *in (Astro)Physics*

Lecture 9: Persuasive Writing I
Telescope / Supercomputing time proposals

Today's lecture

The importance of proposals

The selection process

The structure and content of a typical proposal

Tips for winning proposals



"OUR PROPOSAL DIDN'T GET THE GRANT, BUT THEY
WANT US TO TEACH PROPOSAL WRITING."

The importance of proposals

PROPOSAL WRITING IS A KEY SKILL IN ACADEMIA.

The number of proposals you contribute to/lead a year varies from person to person; it can be as few as 1-2, or up to 10 or more!

A typical proposal can take a few weeks to a few months to write. You will spend a significant amount of time writing/honing each proposal.

The competition is fierce!



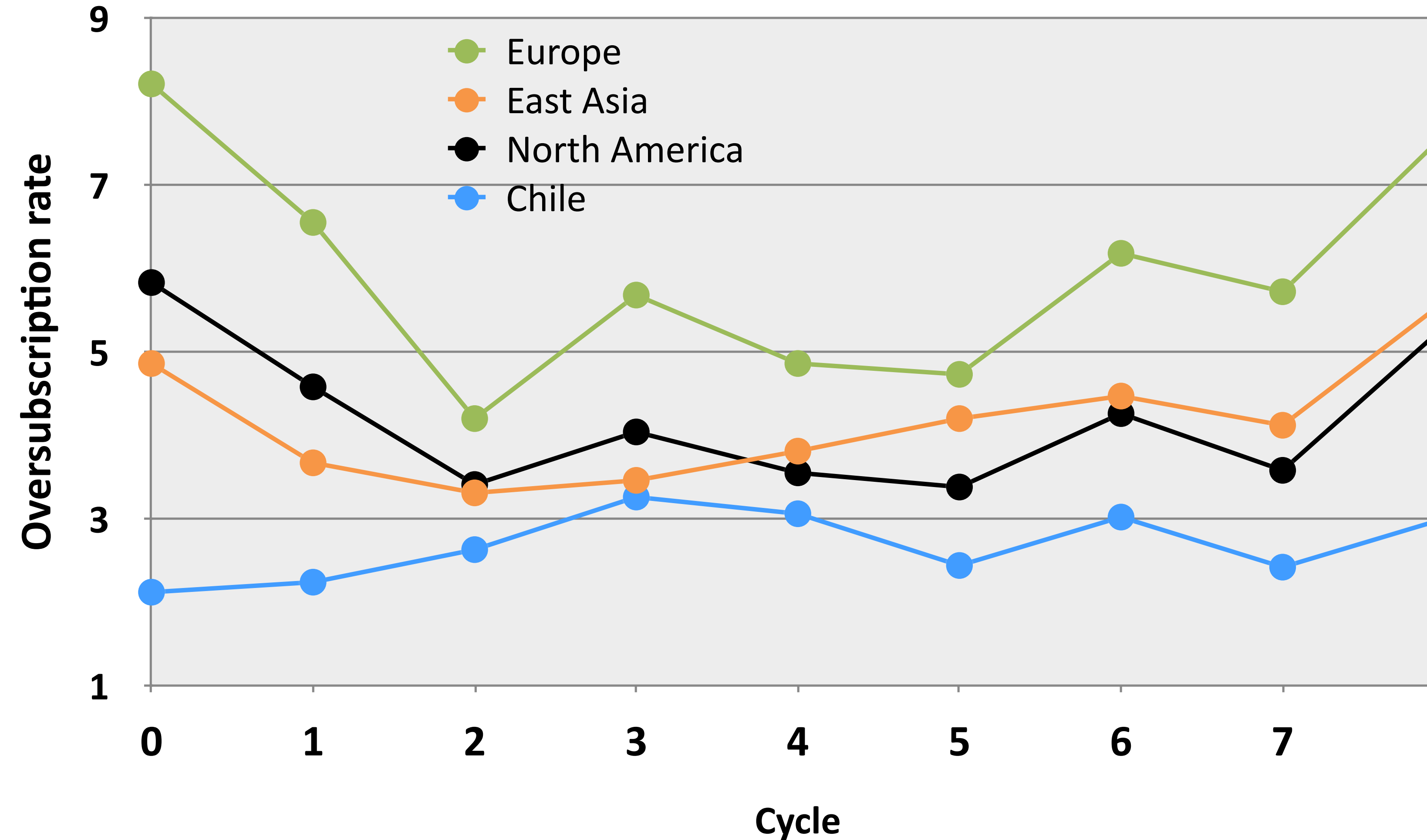
"Is it just me or are these review panels getting a lot tougher?"

Telescope/supercomputing facilities are expensive. You need to **persuade** the time allocation committee (TAC) that your science/project is too pivotal to reject.

For example, only 20% of ESO large programme applications are successful, and ESO telescopes are over-subscribed by >3.



Oversubscription rate by cycle: 12-m Array



Atacama Large Millimetre Array (ALMA)

Building cost: USD \$1.5 billion = AUD \$2.2 billion [not included in the estimate]

Op — Operating costs: USD \$120 million/year = AUD \$179 million/year [1 USD = 1.49 AUD]

N_{hrs} — 4,300 hours of available observing time per cycle (year)

1 hour observing time = Op / N_{hrs} = AUD \$41,630

James Webb Space Telescope (JWST)

Building cost: USD \$10 billion = AUD \$15 billion [not included in the estimate]

Op — Operating costs: USD \$119.6 million/year = AUD \$178.5 million/year

N_{hrs} — 7,000 hours of available observing time per cycle (year)

1 hour observing time = Op / N_{hrs} = AUD \$25,500

ESO Very Large Telescope (VLT)

Building cost: EUR \$330 million = AUD \$511 million [not included in the estimate]

Op — Operating costs: EUR \$59,400/night = AUD \$91,830/night [1 EUR = 1.55 AUD]

N_{hrs} — 8.25 hours observing time / night

1 hour observing time = Op / N_{hrs} = AUD \$11,130



Atacama Large Millimetre Array (ALMA)

Building cost: USD \$1.5 billion = AUD \$2.2 billion [not included in the estimate]

Op — Operating costs: USD \$120 million/year = AUD \$179 million/year [1 USD = 1.49 AUD]

N_{hrs} — 4,300 hours of available observing time per cycle (year)

1 hour observing time = Op / N_{hrs} = AUD \$41,630

James Webb Space Telescope (JWST)

Building cost: USD \$10 billion = AUD \$15 billion [not included in the estimate]

Op — Operating costs: USD \$119.6 million/year = AUD \$178.5 million/year

N_{hrs} — 7,000 hours of available observing time per cycle (year)

1 hour observing time = Op / N_{hrs} = AUD \$25,500

ESO Very Large Telescope (VLT)

Building cost: EUR \$330 million = AUD \$511 million [not included in the estimate]

Op — Operating costs: EUR \$59,400/night = AUD \$91,830/night [1 EUR = 1.55 AUD]

N_{hrs} — 8.25 hours observing time / night

1 hour observing time = Op / N_{hrs} = AUD \$11,130

Cost/hr *usually* less for supercomputing facilities. But competition expands to other fields and industry.

Gadi (National Computing Infrastructure, Australia)

250K CPU cores; 640 NVIDIA GPUs

Op — Operating costs: AUD \$22 million/year

N_{hrs} — 1B hours of compute time per year

1K CPU hours (kSU) = Op / N_{hrs} = AUD \$22 / kSU



The power of persuasion

In an ideal world, the outcome of your proposal would be based solely on the strength of your research idea.

BUT if you have communicated your idea poorly, not followed formatting guidelines, or have not spent sufficient time justifying why you need the resources, the proposal will likely be rejected.

This could severely impact your research and future job prospects.



Isaac Newton struggles to write the economic impact section of his 'gravity' proposal.

The call for proposals

The European Southern Observatory (ESO) has released the Call for Proposals for Period 111 (for observations between 1 April – 30 September 2023). Under the terms of the Strategic Partnership between ESO and Australia, Australian-based astronomers have access to the facilities of the La Silla and Paranal Observatories, specifically the:

- 3.6-m telescope ([3.6](#))
- New Technology Telescope ([NTT](#))
- Very Large Telescope ([VLT](#))
- Very Large Telescope Interferometer ([VLTI](#)).

The proposal deadline is **Tuesday 27 September 2022 at noon Central European Summer Time** (8pm Australian Eastern Standard Time, 6pm Australian Western Standard Time).

Complete details on how to apply can be found at the [P111 Call for Proposals web page](#). All applicants should consult the [Call for Proposals document for Period 111](#), and are required to update their [ESO User Portal](#) accounts to submit or be on proposals.

A wealth of information for Australian applicants can be found on AAL's [Australian ESO Forum](#). Any questions about policies or the practical aspects of proposal preparation should be addressed to the ESO Observing Programmes Office, opo@eso.org. Applicants who may wish to seek advice on proposal or observing strategies, optimal choice of instrument, etc. are invited to contact AAL's ESO Program Manager at Stuart.Ryder@astronomyaustralia.org.au.

Supercomputing Merit Allocations for 2023

Supercomputing Merit Allocation Schemes for 2023 allocation round are now open.

The [National Computational Merit Allocation Scheme \(NCMAS\)](#) is Australia's premiere grant scheme for access to high-performance computing (HPC) resources. The two Tier-1 HPC facilities in Australia, the [National Computational Infrastructure \(NCI\)](#) and the [Pawsey Supercomputing Research Centre](#), together offer hundreds of millions of hours of computing time to meritorious researchers.



The banner features the ALMA logo (a stylized blue and white design) and the text "Atacama Large Millimeter/submillimeter Array" and "In search of our Cosmic Origins". Below the banner is a navigation menu with links: About, Science, Proposing, Observing, Data, Processing, Tools, Documentation, and Help.

ALMA Cycle 10 Call for Proposals

The ALMA Cycle 10 Call for Proposals (CfP) is now closed. The key upcoming dates for the Cycle 10 are given in the following Table.

Date	Milestone
28 June 2023 (15:00 UT)	Deadline to submit reviews for the distributed peer review system
August 2023	Announcement of the outcome of the proposal review process
1 October 2023	Start of ALMA Cycle 10 science observations (anticipated)
30 September 2024	End of ALMA Cycle 10

Before you write...

Read carefully the call for proposals: details on instrument availability and capability/computing capabilities — are the offered capabilities appropriate for your goals?

Consider if you are eligible to apply (for example, Australians cannot be PIs on an ALMA Large Programme; NCMAS proposals cannot be led by an HDR student)

Proposals are team efforts, but as **Principal Investigator** it will be primarily your responsibility to get the document written and submitted.

You shouldn't feel that you need to know all the technical details; this is where **collaborators** come in.

As early career researchers, it is highly advisable to **reach out to more senior researchers**; they will provide a wealth of expertise and their research track record will help bolster the application.

The selection process

TOP-RANKED PROPOSALS ARE AWARDED TIME/MONEY. HOW ARE THEY RANKED?

Step 1: Administrative assessment

Looks at the completeness, compliance, and eligibility of an application. It is important that you don't get rejected at this stage for silly mistakes.

Step 2: Scientific assessment — either a TAC or DPR.

TAC — Time Allocation Committee

Divided into different panels in broad science categories.

Usually 6-8 people per panel (they might not necessarily be experts in your subfield)

Generally, each proposal gets read in detail by at least 2 people: primary & secondary reviewer

Proposals are triaged and discussed at the TAC meeting.

DPR — Distributed Peer Review

Each person who has submitted a proposal as PI reviews and ranks number of proposals (about 10).

Each proposal is independently read and ranked by about 10 people.

The ranks are all combined without further discussion.

A note on the TAC

Bear in mind the mindset
of the TAC

The purpose of the TAC is to boost the scientific return of a facility.

[Advice from the AAO] The TAC will be composed of busy professionals, who have a thousand tasks on their plate. In general, it is best to be cynical and assume:

The TAC will not have a particular expertise in your field and will only be passingly interested in your research (if at all).

The TAC will be impatient.

They don't have enough time to read your proposal thoroughly (so **project summaries/abstracts are all-important**)

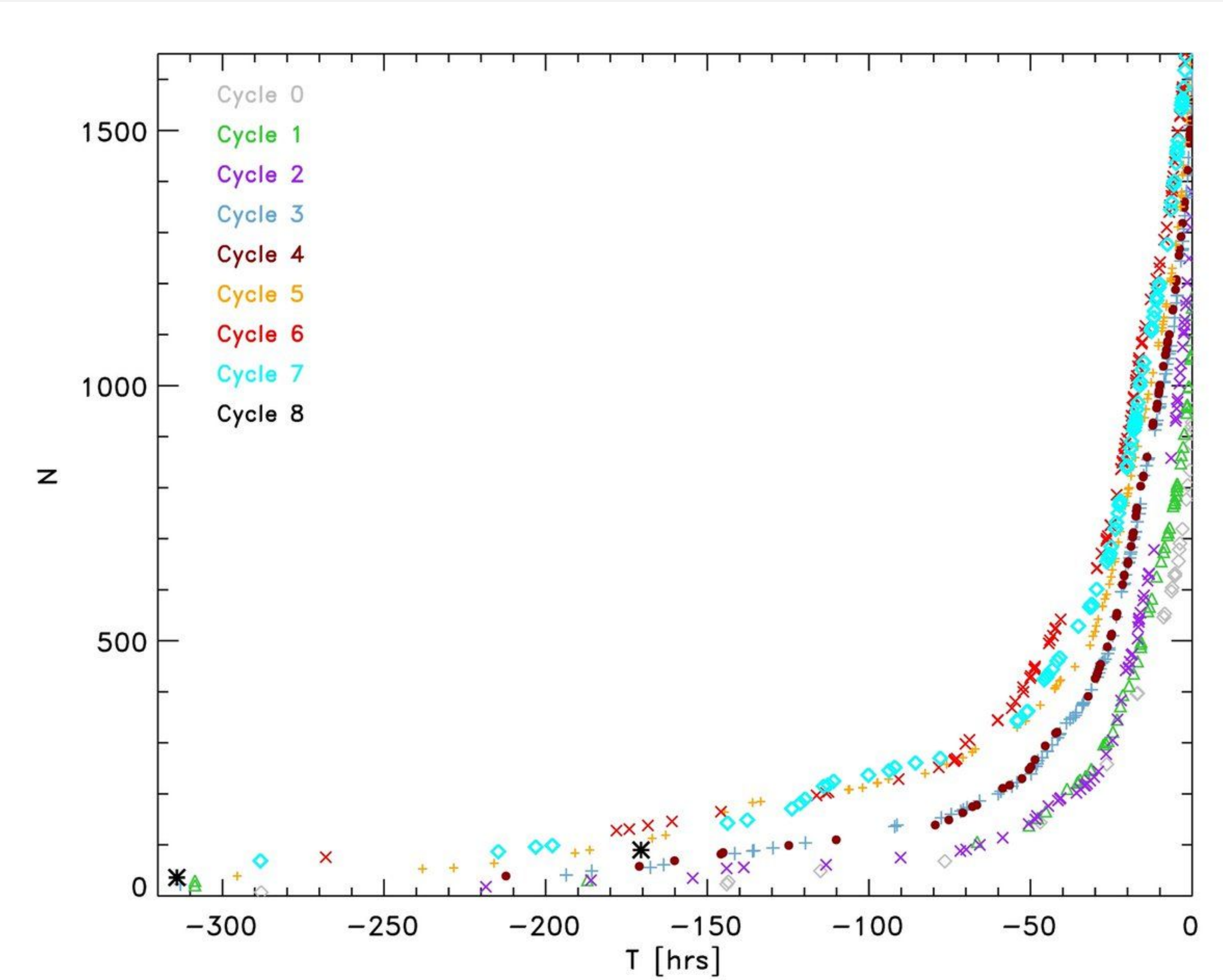
They will be looking for a reason to ignore it.

ULTIMATELY, THE TAC ARE ONLY HUMAN AND YOU WANT TO MAKE THEIR JOB AS EASY AS POSSIBLE.

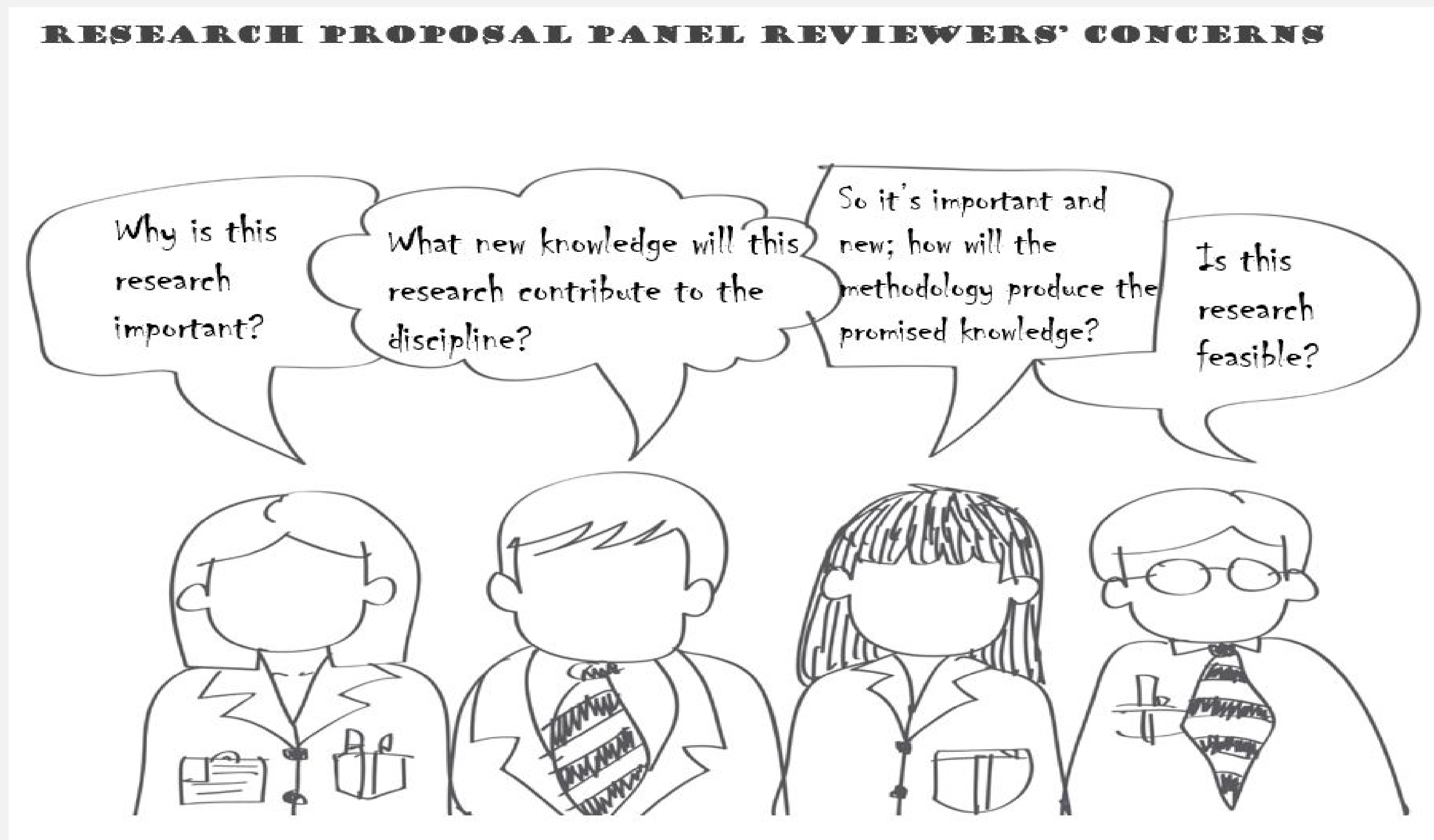
Timing is everything

Don't leave writing your proposal to the last minute, this is when mistakes will happen.

ALMA: number
of submitted
proposals
against time
before the
deadline.



How to write a winning proposal



Structure of a typical proposal

Always follow the structure/template and guidelines specified by each observatory/supercomputing facility.

Always provide all the requested information (read Instructions to Applicants carefully!).

Cover sheet: Includes title and abstract

Scientific Justification (1—4 pages): describe the science case

Technical Justification (1—2 pages): describe the implementation.

Figures, tables, references.

Target list.

IF THE FIRST PAGE ISN'T EXCITING AND EXPLAIN WHAT YOU ARE GOING TO DO, THE PROPOSAL USUALLY GETS REJECTED.

Scientific justification

Good proposals include some **background** on the subject you are studying, in particular **why anyone not in your specific field should care**. Then you can explain **what exactly you want to do**, and **why it will solve every problem left in astronomy** and find a cure for the common cold. Adding **good figures and tables** almost always makes a proposal stronger and easier to understand for the reviewers.

Spitzer Space Telescope Science Center

Scientific justification

Good proposals include some **background** on the subject you are studying, in particular **why anyone not in your specific field should care**. Then you can explain **what exactly you want to do**, and **why it will solve every problem left in astronomy** and find a cure for the common cold. Adding **good figures and tables** almost always makes a proposal stronger and easier to understand for the reviewers.

Spitzer Space Telescope Science Center

What you need to include

Scientific motivation

What is the question you are trying to answer, or the hypothesis you are testing, and why should anyone care?

A justification of resource

Why do you need this facility to do it?

A description of your proposed programme

How are you going to tackle the problem? Exactly what will you do?

A justification of why your team is best placed to tackle the problem

Why you? (though beware dual-anonymous peer review)

Technical justification

Describe the **details of your planned observations**, scheduling constraints, data analysis plans, and how the technical plans were validated.

Include your **estimate of the brightness of your targets**. Based on those brightness estimates, include your estimate and justification of what SNR you expect and how that helps you accomplish your science.

Use **ETCs (exposure time calculators)** and custom observing tools for the facility.

Sometimes a **simulation of what your observation** will look like can be very effective!

For computing proposals, describe memory/storage/processing time requirements of the project. **Details of optimisation tests** should be given here.

<https://www.eso.org/observing/etc/>

<https://asa.alma.cl/SensitivityCalculator/>

<https://jwst/etc.stsci.edu>

Technical justification — include:

Observing:

- Choice of telescope/instrument
- Expected SNR
- Spatial/spectral resolution
- Size of the sample to be observed
- Selection criteria of the proposed targets (remember: statistical significance needs to be quantified)
- Any scheduling constraints (if applicable)

Computing:

- Choice of computing facility
- Storage requirement estimates (both input and results; GB, TB, PB)
- Format of the data (1TB text file not optimised for high performance)
- Optimisation tests (speed, efficiency, output)
- CPU Core / GPU -hour requirement estimates
- Any tests validating the output for the science

Writing a successful proposal

Make your science understandable by a broad audience.

Remember the reviewers might not be in your specific area — make it as easy as possible for the panel to understand your science and proposal. **Give enough general background.**

Get to the point immediately. Readers' attention span is short — grab it early (the hook)

Be explicit — do not assume that the panel will work out what you meant.

Remember: it is likely that your proposal will be the 20th proposal a person reads that day: make it **engaging and easy to follow.**

Avoid jargon, acronyms, and specific terms; if you use them, explain them.

Use figures to emphasize important points / illustrate ideas.

If the reviewer does not understand, you have lost (high oversubscription means they are looking for reasons to reject, not to accept!).

Signals for the reader

Problem/Question/ Unknown	Goals	Strategy	Significance or impact
...has not been determined ...is unclear X is limited by... The question remains whether...	Our goal is... Specifically, we will... Our objective is to... We propose to... We will examine the hypothesis that...	We will achieve this by... Specifically, we will... ...by... We will... Our observing strategy is to...	X will... ...is important for... These results may play a role in... Y can be used to... ultimately... resulting in... ...will provide insights into... This is important because...



Writing a successful proposal

Reviewers/TACs pick up on inconsistencies: write a consistent proposal.

Have you selected the best suited instrument / observing mode for your observations?

Is the requested computation time an appropriate scaling based on optimisation tests?

Are the sample targets and requested exposure times appropriate to achieve the science goals? Note: single-target proposals or proposals targeting large samples need to be especially well justified!

Exposure times have to make sense — use the ETCs.

Figures and tables should help the text and be relevant.

What makes a proposal successful

EXCITING SCIENCE

Providing clear progress in our understanding of some phenomenon.

A NEAT IDEA

Unusual method, original idea, new approach, unique observation or experiment.

CLEAR LANGUAGE

Presents an exciting story, makes it interesting to many people, information to the point.

A CONSISTENT STORY

It's complete and provides all information; quantitative arguments for the amount of time requested.

The Abstract

Write the proposal
abstract first!!!

Note how this is the
opposite of what I
advise for papers!

This is the one paragraph that is guaranteed to be read by everybody.

You have to be able to **summarize the excitement in one paragraph.**

Revisit your abstract several times during the writing and improve it.

Essential parts of a good **executive summary:**

- A sentence with background information and summary of the problem.
- Key information about your request: sample, observing strategy.
- An explanation of what the work will achieve.

The abstract has to contain the punchline!

DOs and DON'Ts

DO put your science into context, so that its relevance for the broader picture, its potential impact, and its timeliness can be appreciated by non-experts in the specific subject of the proposal.

DO be specific about the expected outcome of the project: what quantitative information will be obtained? What physical processes will this information constrain, and how? Will the data be compared to theoretical models (obs. proposal) / new observations (comp. proposal)? Do these support data already exist? If not, when and how will they be developed?

DO fill as accurately and completely as possible all required fields in the proposal form.

DO test-submit your proposal for technical compliance verification as early as possible.

DON'T include post-stamp sized figures (they need to be legible!).

DON'T submit your proposal at the last minute.

DON'T include co-Is without their explicit agreement.

DON'T falsify parameters in the proposal form so as to get unsupported configurations through the proposal verification.

Re-submissions

>35% of ESO proposals are resubmissions. We all have had proposals rejected (and yes, sometimes it really hurts). Pick yourself up and **try again!**

Take into account the feedback from the TAC/reviewers — but don't take it for granted that this guarantees success the next round!

Why did the panel not understand your proposal? This is not only their fault — be more explicit, more direct, crystal clear.

Continuation of previously observed programmes:

- address the new goals
- explain why you need a bigger sample
- what has changed since the last proposal?

Let's look at some examples...

Successful JWST Cycle 1 Proposal

Revealing the hidden stellar emission in the highest-fidelity ALMA-mapped submillimeter galaxies

PI: Hodge, co-PI: da Cunha

ABSTRACT

Twenty years after their discovery, the nature of the most highly star-forming galaxies in the universe remains a mystery. Despite forming stars at 100s-1000s $M_{\odot} \text{ yr}^{-1}$, these $z \sim 2.5$ submillimeter-bright galaxies (SMGs) are notoriously difficult to study with optical telescopes due to their extreme dust obscuration, rendering them faint/invisible even in deep HST H-band imaging, and leading to decades of debate on whether major mergers are necessary to trigger their starbursts. Recently, ALMA has revolutionized the field by revealing the obscured star formation in SMGs in unprecedented detail. Here we propose NIRCam+MIRI imaging at 2-7 μm of 12 SMGs with unrivaled high-S/N ALMA continuum imaging, which span a range in redshift and SFRs reflective of the larger SMG population. By detecting and resolving the stellar emission at rest-frame $\sim 500\text{nm}$ to (crucially) 2 μm — a jump of a factor of 5 in rest-wavelength over the HST H-band — these observations will put first constraints on the underlying morphologies of the stellar emission in these sources, and at a resolution that is perfectly matched to that of the high-S/N ALMA imaging. This proposal will provide maps of resolved stellar mass and star formation rate (and thus, the specific star formation rate), and will yield first reliable total masses for this historically unconstrained population. These observations will provide the context necessary to interpret the ALMA-revealed star formation and its ability to morphologically transform SMGs into their proposed descendants – massive local elliptical galaxies.

Successful ALMA LP Proposal

CRISTAL: a survey of gas, dust and stars on kiloparsec scales in star-forming galaxies at $z \sim 4\text{-}5$

PI: Herrera-Camus

ABSTRACT

ALMA has revolutionized our ability to characterize the cold gas and dust in distant galaxies, enabling pathfinding studies on global scales matched by premier observatories at other wavelengths. With deep HST imaging and the imminent launch of JWST, we are entering an era where stars and warm gas are studied in detail on kiloparsec scales. In this context we propose to carry out the CRISTAL Large Program, making good on one of the key design goals of ALMA to study early galaxies in [CII] emission on highly resolved scales. CRISTAL targets 19 typical $z \sim 4\text{-}5$ galaxies at kiloparsec physical resolution spanning a factor of 30 in stellar mass, and will produce detailed kinematic and morphological maps of the cool gas in and surrounding these galaxies. CRISTAL will provide the next leap forward and a lasting legacy in high-redshift galaxy kinematics, galactic outflows and halos, and ISM properties. CRISTAL enables the next frontier of multiwavelength resolved galaxy studies, combining ALMA, HST, and imminently JWST observations to understand the detailed physics of galaxy formation, the baryon cycle, and the connections between gas, dust, stars, and star formation.

Successful ALMA Proposal

Through the magnifying glass: a unique view of the low-metallicity ISM at high redshift

PI: da Cunha

ABSTRACT

Low-mass galaxies produce up to half of the new stars at the heyday of galaxy formation, yet our knowledge of the physical processes at this epoch is almost solely based on extrapolations from either lower redshifts or higher-mass galaxies. An exceptionally rare lensing configuration has 30-fold magnified a dwarf starburst galaxy at $z=1.847$, providing a unique opportunity to explore the ISM conditions in this important but thus far unobservable regime of galaxy evolution. We propose to take advantage of the magnification of the lensed galaxy SL2SJ02176-0513, a 10% solar metallicity, 10^8 Msol dwarf galaxy with a star formation rate of 10 Msol/yr , combined with the unmatched resolution and sensitivity of ALMA, to obtain the first [CII] map of a metal-poor, high-redshift galaxy at $\sim 150 \text{ pc}$ resolution. By combining this information with existing 0.20 arcsec-resolution UV and emission line maps from HST, we will verify if and how the [CII] line traces star formation in young galaxies. These observations will provide the first ever spatially and kinematically resolved study of the cold ISM in a low-metallicity galaxy at an epoch when the Universe was only a third of its current age.

Scientific Justification

Through the magnifying glass: a unique view of the low-metallicity ISM at high redshift¹

Introduction: a gravitationally-lensed, metal-poor dwarf galaxy at the peak of cosmic star formation

Extensive look-back galaxy surveys have revealed that the star formation rate density of the Universe crested at redshifts between 1.5 and 2.5 (e.g. Hopkins & Beacom 2006), and that about half of the stellar mass of the present Universe was already in place at $z \simeq 1.5$. It has become clear that characterizing star-forming galaxies at this key epoch of galaxy build-up is a crucial step towards understanding the evolution of galaxies. The luminosity and stellar mass functions of galaxies at $z \simeq 2$ (Marchesini et al. 2012, Reddy & Steidel 2009, Lee et al. 2012) indicate that up to 50% of all star formation occurring at this epoch takes place in low-mass galaxies ($M_* < 10^9 M_\odot$). Yet, there is basically no spatially-resolved information on the various ISM phases, and the star formation process and locations in such low-mass galaxies at $z \simeq 2$. This makes our understanding of a large part of the star formation occurring at $z \simeq 2$ still very limited to date.

Extremely fortuitously, a low-mass, low-metallicity, star-forming galaxy at $z = 1.847$ in the UDS field (SL2S J02176-0513; at R.A.= 02^h17^m37^s.237, Dec.= −05°13'29".78) happens to be outstandingly gravitationally lensed by a foreground elliptical galaxy at $z = 0.6459$ (Cabanac et al. 2007, Tu et al. 2009) into three bright images that form a striking tangential arc and a counter image (Fig.1). This is an exceptionally rare gravitational lens system (modeled in detail by Tu et al. 2009, Cooray et al. 2011 and our team [Fig.1c]) which, with a total magnification $\mu_{\text{tot}} \simeq 34$ (as discussed in Fig.1), offers a unique view of the background source, and stretches the images of this dwarf galaxy (which, unlensed, would be barely resolved in high-resolution HST imaging) into an arc spanning over 2.5 arcsec. The counter image is marginally resolved in the HST/ACS images, which allows us to place an upper limit on the effective radius of this galaxy of 350 pc. In the arc, multiple images of two individual star-forming clumps can be separated. The spectrum of the SL2SJ02176-0513 arc was observed with the HST/WFC3 G141 grism as part of the 3D-HST survey (P.I. van Dokkum; Brammer et al. 2012a,b), and it shows very strong [OIII], H β , H γ , H δ and [NeIII] emission (Fig.2), which provide unprecedented diagnostics of the ionized ISM in this galaxy. The Balmer line ratios indicate low dust attenuation ($A_V \simeq 0.2$); moreover, the emission line morphology is similar to the UV continuum morphology (traced by the ACS F606W band), which indicates that extinction affects the UV continuum and lines similarly. In Brammer et al. (2012b) we perform a detailed analysis of these emission lines combined with ACS and WFC3 imaging and find that this galaxy has a (de-magnified) stellar mass $\simeq 10^8 M_\odot$, star formation rate $\simeq 10 M_\odot \text{ yr}^{-1}$ and very low gas-phase metallicity, $12 + \log(\text{O/H}) = 7.5$ (i.e. < 10% of solar metallicity). This stellar mass and SFR imply an exceptionally short stellar mass doubling timescale (< 10 Myr), which means that we must be witnessing this galaxy during a phase of strong growth and feedback. In effect, thanks to the large magnification factor, this source appears to the observer as a low-metallicity, $\simeq 400 M_\odot \text{ yr}^{-1}$ starburst.

While this high magnification lensing system is rare, the type of galaxy it has brought into prominent view is not rare at all. Indeed, an important population of low-mass galaxies at $z \simeq 2$ with physical properties similar to the SL2SJ02176-0513 dwarf has been recently uncovered using deep HST/WFC3 observations, and the number of these galaxies in the young Universe may be even higher than initially suggested (van der Wel et al. 2011, Maseda et al. 2013). However, little is known about the details of the star formation process, ISM properties and gas motions for these low-mass galaxies due to their small sizes. **The enormous gravitational lensing magnification of SL2SJ02176-0513 provides a unique opportunity to spatially resolve the star formation and the ISM in an extremely low-mass, starbursting dwarf galaxy at $z \simeq 2$, which would be impossible for non-lensed systems.** This source represents a truly peerless case of a high-redshift dwarf galaxy magnified 34 times and resolved to physical scales ~ 150 pc, thus providing an unpaired window into the low-metallicity ISM of low-mass galaxies at $z \simeq 2$.

This proposal: We propose to take advantage of the unique magnification of SL2SJ02176-0513, combined with the unmatched resolution and sensitivity of ALMA, to obtain a detailed map of the spatial distribution and kinematics of the star-forming ISM in this galaxy (traced by the [CII] line observed in Band 9), at 0.32" resolution and with a 50 km s $^{-1}$ bandwidth, sufficient to resolve the line. The ALMA data will be complemented by deep HST spatially-resolved CANDELS ACS+WFC3 imaging and 3D-HST WFC3 grism spectroscopy with similar spatial resolution already in hand, and an upcoming LBT high-resolution rest-frame optical spectrum. The proposed observations will provide the first-ever detailed study of the physics and the kinematics of the star-forming ISM in an extremely low-metallicity, low-mass galaxy at $z \simeq 2$, an epoch when the Universe was

only a third of its current age. This is the only known dwarf galaxy at that redshift for which we can perform such high sensitivity and spatially-resolved study thanks to the strong gravitational lensing and the outstanding capabilities of ALMA². We stress that even with full capability ALMA will *not* be able to achieve similar data quality for un-lensed systems with similarly low masses. Our ambitious scientific goals can already be achieved in Cycle 3 with a **modest time request of 44 minutes on-source**.

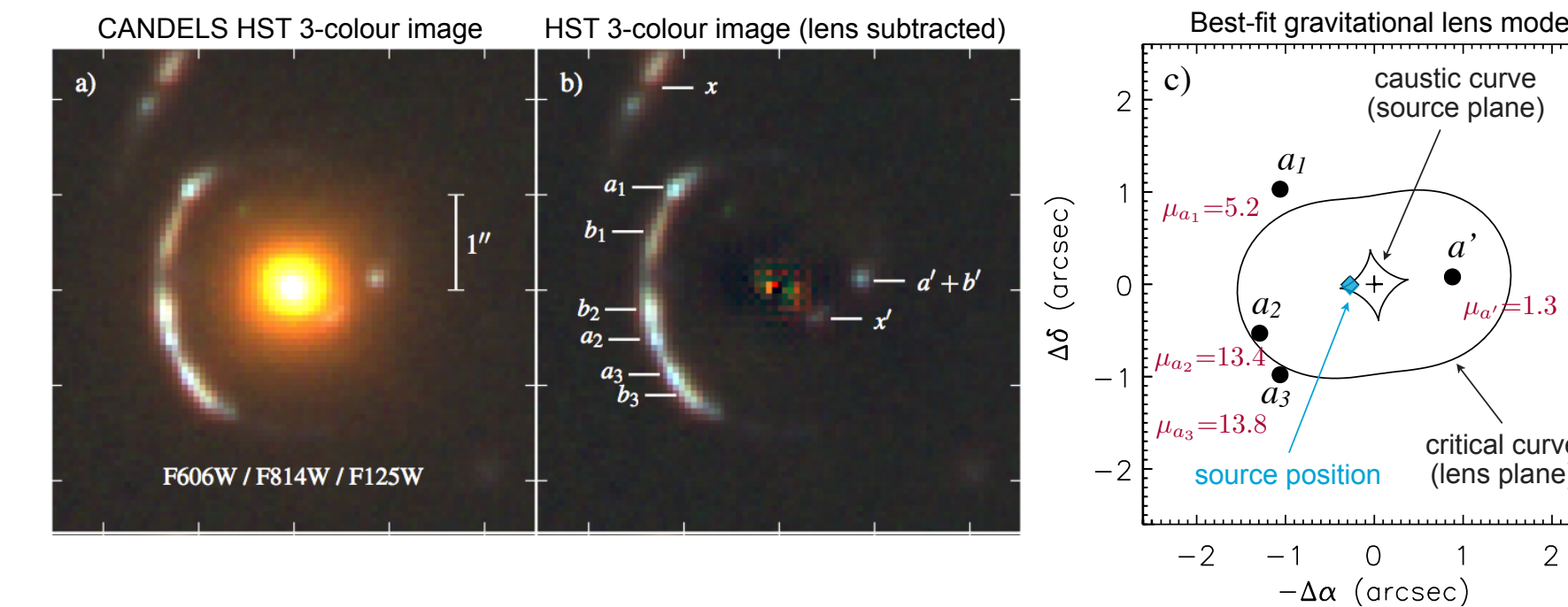


Fig. 1: (a) HST 5'' \times 5'' three-colour image of the SL2SJ02176-0513 gravitational lens system. (b) Same image, with the foreground elliptical lens removed. Our target is the $z = 1.847$ galaxy lensed into the striking arc, showing the distribution of the rest-frame UV/optical light. Several lensed images of two main resolved star-forming clumps in this galaxy can be observed ('a' and 'b' labelled in the arc and in the counter image). The conjugate images of an additional lensed object, 'x', at $z = 2.29$, are also indicated (Brammer et al. 2012b). We do not expect emission from the lens galaxy (an elliptical) to contaminate our observations of the arc. In the unlikely case there is some emission from the lens, the spatial resolution of our observations (0.32") will allow us to cleanly subtract it similarly to what was done in the HST images. (c) Our best-fit gravitational lens model using the method by co-I van de Ven et al. (2010) which produces an analytical lens model that allows for a non-spherical underlying mass distribution of the lens. The model with an isothermal radial slope $\alpha = -1$ for the density profile (consistent with independent modelling by Tu et al. 2009) fits the image positions a_1 , a_2 , a_3 and a' , and yields the individual magnification factors indicated in red; the total magnification for this model is $\mu_{\text{tot}} = 33.7$. We note that while this model provides an excellent fit to the image positions and is consistent with other modelling efforts, the density slope α is less well constrained. We explore a range of realistic values for α between -0.8 and -1.2 , for which the predicted source positions remain well within the errors on the observed positions; these slope values imply total magnifications μ_{tot} between 24.5 and 55.5. **Our proposed [CII] observations will provide a dust-unbiased measure of the flux ratios between the different source images that we will input into our lens modelling to constrain simultaneously the shape and radial slope of the density profile, and thus the total magnification** (van de Ven et al. 2010).

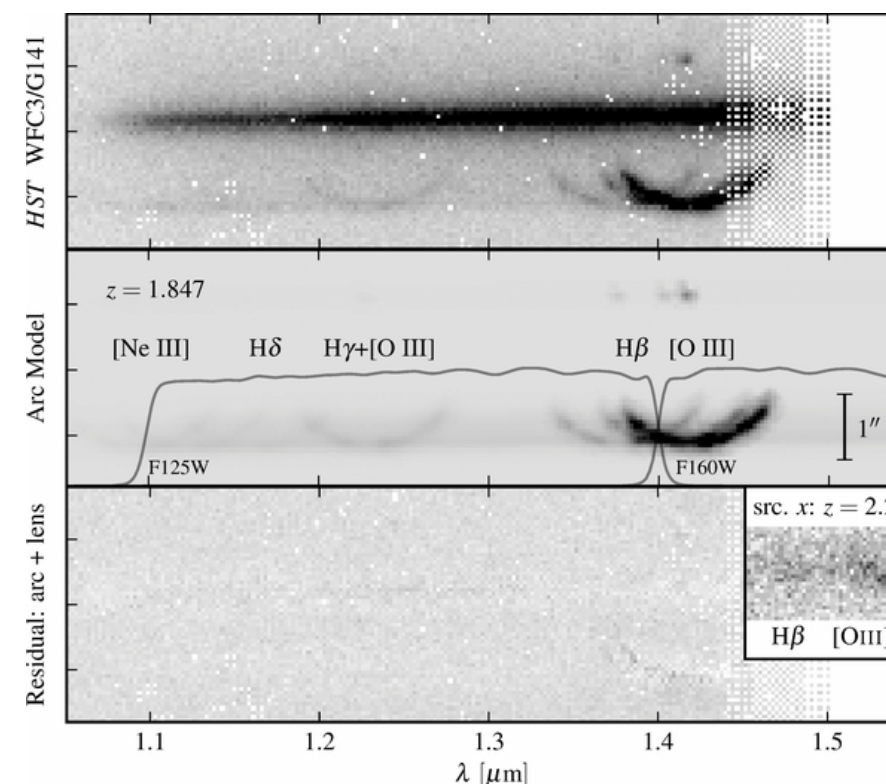


Fig. 2: WFC3/G141 grism spectrum of the SL2SJ02176-0513 lens system from the 3D-HST survey (Brammer et al. 2012a,b). Top panel: combined spectrum of the foreground lens galaxy and the gravitational arc and counter image – the various arc images show spectacular and truly unique diagnostics of the spatial distribution of line emission from HII regions powered by star formation in our target. Middle panel: model where the lens is removed and the lensed two-dimensional spectrum is modelled assuming the line morphology follows the F140W direct image (dominated by the [OIII] line). Bottom panel: residual showing that the model is an excellent reproduction of the observed arc spectrum (Brammer et al. 2012b); the small inset panel shows detections from an adjacent 3D-HST pointing of weak H β and [OIII] emission lines for the other lensed source 'x' (Fig.1) at $z = 2.29$.

²The only other known strongly lensed high-redshift dwarf galaxy (van der Wel et al. 2013) is not a suitable target because (i) the lensing configuration is not as ideal (less gain in spatial resolution and challenging lens subtraction) and (ii) the WFC3 grism spectrum is highly contaminated by the lens, so we do not have the same exquisitely detailed view of the star formation activity, dust attenuation and metallicity.

Proposal goals:

(1) To obtain the first detection and map of the cool, star-forming ISM of a low-metallicity dwarf galaxy at $z \simeq 2$. To trace the star-forming ISM, we propose to observe the 1900.54 GHz [CII] line (at 667.58 GHz i.e. Band 9 for the redshift of our source), which is the brightest, main cooling line of the ISM in star-forming galaxies. This line is believed to arise mainly from photo-dissociation regions (PDRs), which are typically associated with star-forming regions. Since our target is a low-metallicity dwarf, we expect the [CII] line to be exceptionally bright (compared to the infrared and CO): observations of local dwarf galaxies show that low-metallicity environments are characterized by strong UV radiation fields and low dust-to-gas ratios, which cause CO molecules to be less shielded from UV photons and more easily dissociated. This leads to ‘CO-dark’ gas and enhanced [CII]/CO and [CII]/infrared ratios in low-metallicity dwarf galaxies (e.g. Madden et al.1997). This is a likely explanation for the fact that our recent PdBI observations of our source at 81 GHz down to a sensitivity of 0.21 mJy/beam (P.I. Aravena) do not show a CO(2-1) line detection. **Therefore [CII] is an optimal and likely the only possible tracer of the bulk of the star-forming ISM in SL2SJ02176-0513 (and low-metallicity high-redshift dwarf galaxies in general).** Based on studies of local low-metallicity dwarf galaxies (Madden et al.1997, 2000, Cormier et al.2010), we expect the [CII] line luminosity in our source to be at least 1.5% of the infrared luminosity (which based on our sophisticated spectral modelling should be at least $2 \times 10^{11} L_{\odot}$ with magnification; Fig.3), which for a line FWHM of 120 km s $^{-1}$ gives a total velocity-integrated flux of 181 mJy, spread over ~ 10 beams in the C36-2 Cycle 3 configuration (Fig.4). We request a sensitivity of 2 mJy/beam to detect the line with S/N ~ 9 on average along the gravitational arc; Fig.4 shows that this sensitivity is necessary to detect the emission in the faintest parts.

Given its brightness and frequency, the [CII] line has been proposed as an ideal tracer of star formation in high-redshift galaxies ($z \gtrsim 2$) with ALMA (e.g. Stacey et al.2010). However, the low ionization potential of [CII] (11.3 eV), means that it may originate from a broad range of ISM phases, from diffuse HI to HII regions, and the physics and efficacy of this line in tracing SFR are not yet well established. SL2SJ02176-0513 provides a valuable opportunity to test how well [CII] traces star formation in the low-metallicity, high-redshift ISM. Our proposed [CII] line map will be the first ever view of the star-forming ISM in a low-mass, low-metallicity galaxy at $z \simeq 2^3$. We will test how well the [CII] line emission traces the star formation rate by directly comparing our [CII] line map with the exquisite HST data already in hand (Figs.1 & 2), which provide stellar UV/optical continuum and [OIII] and H β emission line maps at similar resolution. Since our target is not strongly affected by dust extinction, these maps provide a complete view of the star formation in the galaxy that can be directly compared with the [CII]. **This analysis be a crucial stepping stone in calibrating the [CII] line as a star formation rate tracer for high-redshift observations with ALMA. In the future, with full ALMA capabilities, we will be able to detect [CII] for a more statistically significant sample of (unlensed) $z \simeq 2$ low-metallicity dwarf galaxies observed in the optical with HST/WFC3, albeit at lower sensitivity and spatial resolution. Hence, the lensed source SL2SJ02176-0513 is a crucial benchmark and opens the window to the low-metallicity Universe at high redshift.**

(2) To measure the kinematics of the star-forming gas. The predicted brightness of the [CII] line implies that we can resolve the lensed source not only spatially but also in velocity space with a modest amount of observing time (44 minutes) with ALMA Cycle 3 capabilities. The requested bandwidth of 111 MHz will provide a resolution of 50 km s $^{-1}$, sufficient to resolve the [CII] line: nebular emission lines in the optical have velocity dispersions of 50 km s $^{-1}$ (FWHM 120 km s $^{-1}$) for this class of objects (Maseda et al.2013). The measured velocity dispersion will allow us to estimate the galaxy’s dynamical mass and, combined with the known stellar mass, its gas fraction. The [CII] line is likely to trace a more dynamically relaxed phase of the ISM than the high excitation emission lines observed in the optical. Therefore, the [CII] line will provide our best estimate of the systemic velocity of the galaxy. **We will compare this velocity with the velocity of high excitation optical lines tracing the ionized ISM from an upcoming LBT/LUCI optical spectrum of our galaxy with matched velocity resolution to look for outflows of ionized gas powered by the intense starburst in this dwarf galaxy.**

³Similar Cycle 0 ALMA spatially-resolved [CII] observations of a gravitationally-lensed, star-forming $z \simeq 2$ galaxy recently published by Schaefer et al.(2015) demonstrate that our proposed observations are technically feasible. We stress that the science addressed with our proposal is different, since we will probe the low-mass, metal-poor regime (mass of our target is over an order of magnitude smaller), and we have additional UV and optical emission-line observations from HST that will allow us to perform a more detailed analysis of the spatial distribution of star formation and ISM properties in our target.

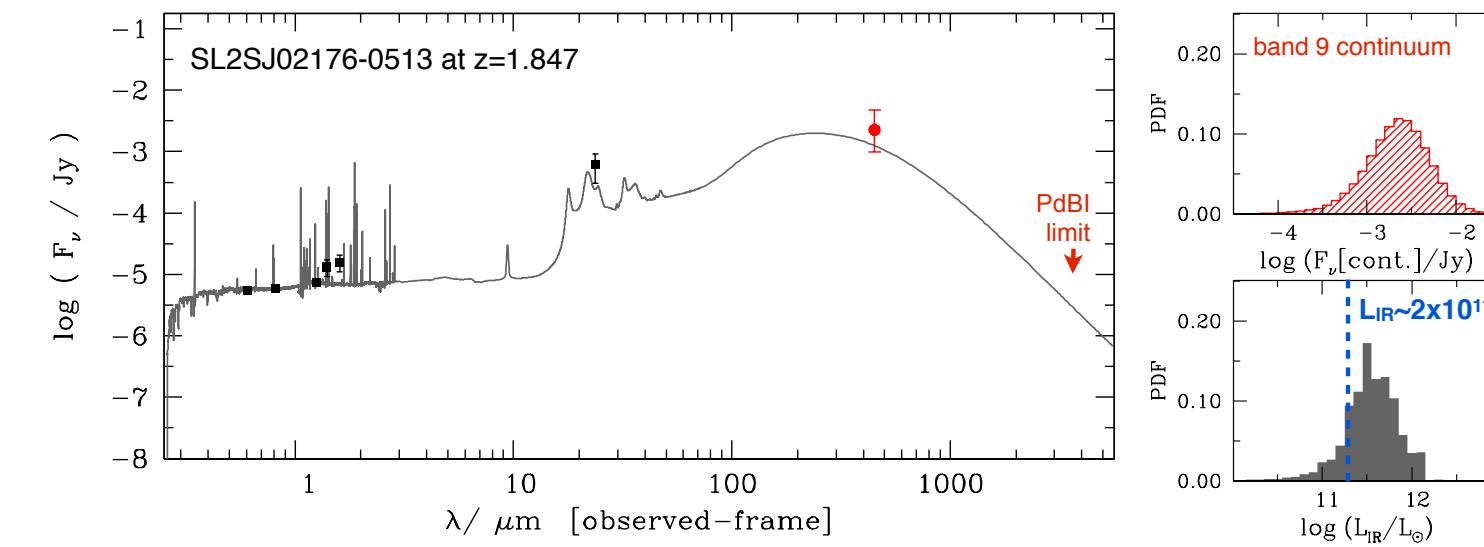


Fig. 3: Fit to the (magnified) spectral energy distribution (SED) of our lensed low-mass galaxy. Black points: observed fluxes (including the marginal MIPS 24- μ m detection); red point: predicted Band-9 continuum flux; red arrow: continuum sensitivity reached by our PdBI observations at $\simeq 80$ GHz (23 mJy). We include the emission line flux in the broad bands (using the models by Pacifici et al.2012) and compute the infrared SED consistently with the inferred dust attenuation of the continuum + lines in terms of energy balance using the MAGPHYS model (da Cunha et al.2008). We derive Bayesian likelihood distributions for the total infrared luminosity L_{IR} and the 158 μ m continuum – we incorporate our uncertainties due to the lack of data in the far-IR by marginalizing over a large library of dust emission models with different PAHs contributions and dust temperatures (da Cunha et al.2013). This allows us to derive robust, physically-consistent estimates for the expected total dust luminosity (and hence [CII] luminosity) and Band-9 continuum flux for our galaxy. We take a (conservative) estimate of $L_{\text{IR}} = 2 \times 10^{11} L_{\odot}$ (not corrected for lensing).

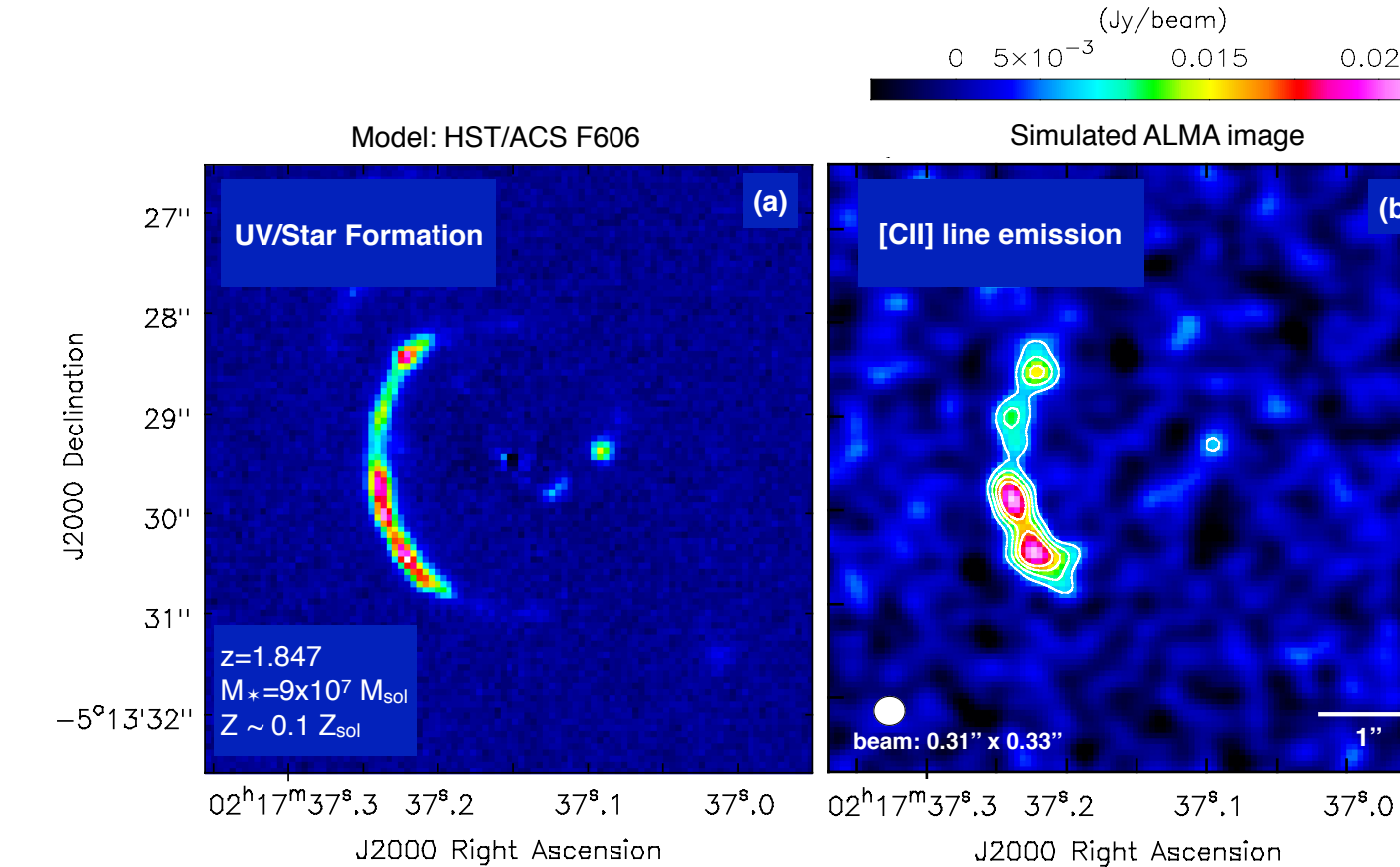


Fig. 4: CASA simulated ALMA [CII] line map of SL2SJ02176-0513 at $\sim 0.3''$ resolution (Cycle 3 C36-2 antenna configuration), 111 MHz bandwidth at 667.58 GHz, 2 mJy/beam rms (total 44 minutes on-source). (a) Input model: HST/ACS F606W image at 0.2'' resolution, mapping the rest-frame UV emission; (b) Simulated [CII] map (including noise); the contours show the 3-, 5-, 7- and 9- σ levels. This shows that the requested sensitivity of 2 mJy/beam is needed to detect the faintest regions of the arc (if the [CII] emission is distributed in the same way as the star formation rate).

Potential for publicity: These observations will produce unique, highly significant results that we plan to publish within six months of obtaining the data, along with press-release quality images of the star formation and ISM of the most distant, low-mass, metal-poor galaxy ever observed. The combination of the stunning gravitational arc and the detailed view of such a young galaxy in the early Universe will surely capture people’s imagination, and demonstrate the outstanding capabilities of ALMA to a broad public.

- References**
- Brammer, G. B., et al. 2012a, ApJS 200,13; 2012b, ApJL 758, 17 • Cabanac, R. A., et al. 2007, A&A 461, 813
 - Cooray, A., et al. 2011, arXiv:1110.3784 • Cormier, D., et al. 2010, A&A 517, L57 • da Cunha, E., et al. 2008, MNRAS 388, 1595; 2013, ApJ 765, 9 • Hopkins, A. M. & Beacom, J. F. 2006, ApJ 651, 142 • Lee, K.-S., et al. 2012, ApJ 752, 66 • Madden, S., et al. 1997, ApJ 483, 200 • Madden, S. 2000, New Astron. Rev. 44, 249 • Marchesini, D., et al. 2012, ApJ 748, 126 • Maseda, M. V., et al. 2013, ApJL 778, 22 • Pacifici, C., et al. 2012, MNRAS 421, 2002 • Reddy, N. A. & Steidel, C. C. 2009, ApJ 692, 813 • Schaefer, D., et al. 2015, A&A 576, L2 • Stacey, G., et al. 2010, ApJ 724, 957 • Tu, H., et al. 2009, A&A 501, 475 • van der Ven, G., et al. 2010, ApJ 719, 1481 • van der Wel, A., et al. 2011, ApJ 742, 111; 2013, ApJL 777, 17

Through the magnifying glass: a unique view of the low-metallicity ISM at high redshift¹

Introduction: a gravitationally-lensed, metal-poor dwarf galaxy at the peak of cosmic star formation

Extensive look-back galaxy surveys have revealed that the star formation rate density of the Universe crested at redshifts between 1.5 and 2.5 (e.g. Hopkins & Beacom 2006), and that about half of the stellar mass of the present Universe was already in place at $z \simeq 1.5$. It has become clear that characterizing star-forming galaxies at this key epoch of galaxy build-up is a crucial step towards understanding the evolution of galaxies. The luminosity and stellar mass functions of galaxies at $z \simeq 2$ (Marchesini et al. 2012, Reddy & Steidel 2009, Lee et al. 2012) indicate that up to 50% of all star formation occurring at this epoch takes place in low-mass galaxies ($M_* < 10^9 M_\odot$). Yet, there is basically no spatially-resolved information on the various ISM phases, and the star formation process and locations in such low-mass galaxies at $z \simeq 2$. This makes our understanding of a large part of the star formation occurring at $z \simeq 2$ still very limited to date.

Extremely fortuitously, a low-mass, low-metallicity, star-forming galaxy at $z = 1.847$ in the UDS field (SL2S J02176-0513; at R.A.= 02^h17^m37^s.237, Dec.= $-05^\circ 13' 29''.78$) happens to be outstandingly gravitationally lensed by a foreground elliptical galaxy at $z = 0.6459$ (Cabanac et al. 2007, Tu et al. 2009) into three bright images that form a striking tangential arc and a counter image (Fig.1). This is an exceptionally rare gravitational lens system (modeled in detail by Tu et al. 2009, Cooray et al. 2011 and our team [Fig.1c]) which, with a total magnification $\mu_{\text{tot}} \simeq 34$ (as discussed in Fig.1), offers a unique view of the background source, and stretches the images of this dwarf galaxy (which, unlensed, would be barely resolved in high-resolution HST imaging) into an arc spanning over 2.5 arcsec. The counter image is marginally resolved in the HST/ACS images, which allows us to place an upper limit on the effective radius of this galaxy of 350 pc. In the arc, multiple images of two individual star-forming clumps can be separated. The spectrum of the SL2SJ02176-0513 arc was observed with the HST/WFC3 G141 grism as part of the 3D-HST survey (P.I. van Dokkum; Brammer et al. 2012a,b), and it shows very strong [OIII], H β , H γ , H δ and [NeIII] emission (Fig.2), which provide unprecedented diagnostics of the ionized ISM in this galaxy. The Balmer line ratios indicate low dust attenuation ($A_V \simeq 0.2$); moreover, the emission line morphology is similar to the UV continuum morphology (traced by the ACS F606W band), which indicates that extinction affects the UV continuum and lines similarly. In Brammer et al. (2012b) we perform a detailed analysis of these emission lines combined with ACS and WFC3 imaging and find that this galaxy has a (de-magnified) stellar mass $\simeq 10^8 M_\odot$, star formation rate $\simeq 10 M_\odot \text{ yr}^{-1}$ and very low gas-phase metallicity, $12 + \log(\text{O/H}) = 7.5$ (i.e. $< 10\%$ of solar metallicity). This stellar mass and SFR imply an exceptionally short stellar mass doubling timescale (< 10 Myr), which means that we must be witnessing this galaxy during a phase of strong growth and feedback. In effect, thanks to the large magnification factor, this source appears to the observer as a low-metallicity, $\simeq 400 M_\odot \text{ yr}^{-1}$ starburst.

While this high magnification lensing system is rare, the type of galaxy it has brought into prominent view is not rare at all. Indeed, an important population of low-mass galaxies at $z \simeq 2$ with physical properties similar to the SL2SJ02176-0513 dwarf has been recently uncovered using deep HST/WFC3 observations, and the number of these galaxies in the young Universe may be even higher than initially suggested (van der Wel et al. 2011, Maseda et al. 2013). However, little is known about the details of the star formation process, ISM properties and gas motions for these low-mass galaxies due to their small sizes. **The enormous gravitational lensing magnification of SL2SJ02176-0513 provides a unique opportunity to spatially resolve the star formation and the ISM in an extremely low-mass, starbursting dwarf galaxy at $z \simeq 2$, which would be impossible for non-lensed systems.** This source represents a truly peerless case of a high-redshift dwarf galaxy magnified 34 times and resolved to physical scales ~ 150 pc, thus providing an unpaired window into the low-metallicity ISM of low-mass galaxies at $z \simeq 2$.

This proposal: We propose to take advantage of the unique magnification of SL2SJ02176-0513, combined with the unmatched resolution and sensitivity of ALMA, to obtain a detailed map of the spatial distribution and kinematics of the star-forming ISM in this galaxy (traced by the [CII] line observed in Band 9), at 0.32'' resolution and with a 50 km s^{-1} bandwidth, sufficient to resolve the line. The ALMA data will be complemented by deep HST spatially-resolved CANDELS ACS+WFC3 imaging and 3D-HST WFC3 grism spectroscopy with similar spatial resolution already in hand, and an upcoming LBT high-resolution rest-frame optical spectrum. The proposed observations will provide the first-ever detailed study of the physics and the kinematics of the star-forming ISM in an extremely low-metallicity, low-mass galaxy at $z \simeq 2$, an epoch when the Universe was

Through the magnifying glass: a unique view of the low-metallicity ISM at high redshift¹

Introduction: a gravitationally-lensed, metal-poor dwarf galaxy at the peak of cosmic star formation

Extensive look-back galaxy surveys have revealed that the star formation rate density of the Universe crested at redshifts between 1.5 and 2.5 (e.g. Hopkins & Beacom 2006), and that about half of the stellar mass of the present Universe was already in place at $z \simeq 1.5$. It has become clear that characterizing star-forming galaxies at this key epoch of galaxy build-up is a crucial step towards understanding the evolution of galaxies. The luminosity and stellar mass functions of galaxies at $z \simeq 2$ (Marchesini et al. 2012, Reddy & Steidel 2009, Lee et al. 2012) indicate that up to 50% of all star formation occurring at this epoch takes place in low-mass galaxies ($M_* < 10^9 M_\odot$). Yet, there is basically no spatially-resolved information on the various ISM phases, and the star formation process and locations in such low-mass galaxies at $z \simeq 2$. This makes our understanding of a large part of the star formation occurring at $z \simeq 2$ still very limited to date.

Extremely fortuitously, a low-mass, low-metallicity, star-forming galaxy at $z = 1.847$ in the UDS field (SL2S J02176-0513; at R.A.= 02^h17^m37^s.237, Dec.= $-05^\circ 13' 29''.78$) happens to be outstandingly gravitationally lensed by a foreground elliptical galaxy at $z = 0.6459$ (Cabanac et al. 2007, Tu et al. 2009) into three bright images that form a striking tangential arc and a counter image (Fig.1). This is an exceptionally rare gravitational lens system (modeled in detail by Tu et al. 2009, Cooray et al. 2011 and our team [Fig.1c]) which, with a total magnification $\mu_{\text{tot}} \simeq 34$ (as discussed in Fig.1), offers a unique view of the background source, and stretches the images of this dwarf galaxy (which, unlensed, would be barely resolved in high-resolution HST imaging) into an arc spanning over 2.5 arcsec. The counter image is marginally resolved in the HST/ACS images, which allows us to place an upper limit on the effective radius of this galaxy of 350 pc. In the arc, multiple images of two individual star-forming clumps can be separated. The spectrum of the SL2SJ02176-0513 arc was observed with the HST/WFC3 G141 grism as part of the 3D-HST survey (P.I. van Dokkum; Brammer et al. 2012a,b), and it shows very strong [OIII], H β , H γ , H δ and [NeIII] emission (Fig.2), which provide unprecedented diagnostics of the ionized ISM in this galaxy. The Balmer line ratios indicate low dust attenuation ($A_V \simeq 0.2$); moreover, the emission line morphology is similar to the UV continuum morphology (traced by the ACS F606W band), which indicates that extinction affects the UV continuum and lines similarly. In Brammer et al. (2012b) we perform a detailed analysis of these emission lines combined with ACS and WFC3 imaging and find that this galaxy has a (de-magnified) stellar mass $\simeq 10^8 M_\odot$, star formation rate $\simeq 10 M_\odot \text{ yr}^{-1}$ and very low gas-phase metallicity, $12 + \log(\text{O/H}) = 7.5$ (i.e. $< 10\%$ of solar metallicity). This stellar mass and SFR imply an exceptionally short stellar mass doubling timescale (< 10 Myr), which means that we must be witnessing this galaxy during a phase of strong growth and feedback. In effect, thanks to the large magnification factor, this source appears to the observer as a low-metallicity, $\simeq 400 M_\odot \text{ yr}^{-1}$ starburst.

While this high magnification lensing system is rare, the type of galaxy it has brought into prominent view is not rare at all. Indeed, an important population of low-mass galaxies at $z \simeq 2$ with physical properties similar to the SL2SJ02176-0513 dwarf has been recently uncovered using deep HST/WFC3 observations, and the number of these galaxies in the young Universe may be even higher than initially suggested (van der Wel et al. 2011, Maseda et al. 2013). However, little is known about the details of the star formation process, ISM properties and gas motions for these low-mass galaxies due to their small sizes. **The enormous gravitational lensing magnification of SL2SJ02176-0513 provides a unique opportunity to spatially resolve the star formation and the ISM in an extremely low-mass, starbursting dwarf galaxy at $z \simeq 2$, which would be impossible for non-lensed systems.** This source represents a truly peerless case of a high-redshift dwarf galaxy magnified 34 times and resolved to physical scales ~ 150 pc, thus providing an unpaired window into the low-metallicity ISM of low-mass galaxies at $z \simeq 2$.

This proposal: We propose to take advantage of the unique magnification of SL2SJ02176-0513, combined with the unmatched resolution and sensitivity of ALMA, to obtain a detailed map of the spatial distribution and kinematics of the star-forming ISM in this galaxy (traced by the [CII] line observed in Band 9), at 0.32'' resolution and with a 50 km s^{-1} bandwidth, sufficient to resolve the line. The ALMA data will be complemented by deep HST spatially-resolved CANDELS ACS+WFC3 imaging and 3D-HST WFC3 grism spectroscopy with similar spatial resolution already in hand, and an upcoming LBT high-resolution rest-frame optical spectrum. The proposed observations will provide the first-ever detailed study of the physics and the kinematics of the star-forming ISM in an extremely low-metallicity, low-mass galaxy at $z \simeq 2$, an epoch when the Universe was

Through the magnifying glass: a unique view of the low-metallicity ISM at high redshift¹

Introduction: a gravitationally-lensed, metal-poor dwarf galaxy at the peak of cosmic star formation

Extensive look-back galaxy surveys have revealed that the star formation rate density of the Universe crested at redshifts between 1.5 and 2.5 (e.g. Hopkins & Beacom 2006), and that about half of the stellar mass of the present Universe was already in place at $z \simeq 1.5$. It has become clear that characterizing star-forming galaxies at this key epoch of galaxy build-up is a crucial step towards understanding the evolution of galaxies. The luminosity and stellar mass functions of galaxies at $z \simeq 2$ (Marchesini et al. 2012, Reddy & Steidel 2009, Lee et al. 2012) indicate that up to 50% of all star formation occurring at this epoch takes place in low-mass galaxies ($M_* < 10^9 M_\odot$). Yet, there is basically no spatially-resolved information on the various ISM phases, and the star formation process and locations in such low-mass galaxies at $z \simeq 2$. This makes our understanding of a large part of the star formation occurring at $z \simeq 2$ still very limited to date.

Extremely fortuitously, a low-mass, low-metallicity, star-forming galaxy at $z = 1.847$ in the UDS field (SL2S J02176-0513; at R.A.= 02^h17^m37^s.237, Dec.= $-05^\circ 13' 29''.78$) happens to be outstandingly gravitationally lensed by a foreground elliptical galaxy at $z = 0.6459$ (Cabanac et al. 2007, Tu et al. 2009) into three bright images that form a striking tangential arc and a counter image (Fig.1). This is an exceptionally rare gravitational lens system (modeled in detail by Tu et al. 2009, Cooray et al. 2011 and our team [Fig.1c]) which, with a total magnification $\mu_{\text{tot}} \simeq 34$ (as discussed in Fig.1), offers a unique view of the background source, and stretches the images of this dwarf galaxy (which, unlensed, would be barely resolved in high-resolution HST imaging) into an arc spanning over 2.5 arcsec. The counter image is marginally resolved in the HST/ACS images, which allows us to place an upper limit on the effective radius of this galaxy of 350 pc. In the arc, multiple images of two individual star-forming clumps can be separated. The spectrum of the SL2SJ02176-0513 arc was observed with the HST/WFC3 G141 grism as part of the 3D-HST survey (P.I. van Dokkum; Brammer et al. 2012a,b), and it shows very strong [OIII], H β , H γ , H δ and [NeIII] emission (Fig.2), which provide unprecedented diagnostics of the ionized ISM in this galaxy. The Balmer line ratios indicate low dust attenuation ($A_V \simeq 0.2$); moreover, the emission line morphology is similar to the UV continuum morphology (traced by the ACS F606W band), which indicates that extinction affects the UV continuum and lines similarly. In Brammer et al. (2012b) we perform a detailed analysis of these emission lines combined with ACS and WFC3 imaging and find that this galaxy has a (de-magnified) stellar mass $\simeq 10^8 M_\odot$, star formation rate $\simeq 10 M_\odot \text{ yr}^{-1}$ and very low gas-phase metallicity, $12 + \log(\text{O/H}) = 7.5$ (i.e. $< 10\%$ of solar metallicity). This stellar mass and SFR imply an exceptionally short stellar mass doubling timescale (< 10 Myr), which means that we must be witnessing this galaxy during a phase of strong growth and feedback. In effect, thanks to the large magnification factor, this source appears to the observer as a low-metallicity, $\simeq 400 M_\odot \text{ yr}^{-1}$ starburst.

While this high magnification lensing system is rare, the type of galaxy it has brought into prominent view is not rare at all. Indeed, an important population of low-mass galaxies at $z \simeq 2$ with physical properties similar to the SL2SJ02176-0513 dwarf has been recently uncovered using deep HST/WFC3 observations, and the number of these galaxies in the young Universe may be even higher than initially suggested (van der Wel et al. 2011, Maseda et al. 2013). However, little is known about the details of the star formation process, ISM properties and gas motions for these low-mass galaxies due to their small sizes. **The enormous gravitational lensing magnification of SL2SJ02176-0513 provides a unique opportunity to spatially resolve the star formation and the ISM in an extremely low-mass, starbursting dwarf galaxy at $z \simeq 2$, which would be impossible for non-lensed systems.** This source represents a truly peerless case of a high-redshift dwarf galaxy magnified 34 times and resolved to physical scales ~ 150 pc, thus providing an unpaired window into the low-metallicity ISM of low-mass galaxies at $z \simeq 2$.

This proposal: We propose to take advantage of the unique magnification of SL2SJ02176-0513, combined with the unmatched resolution and sensitivity of ALMA, to obtain a detailed map of the spatial distribution and kinematics of the star-forming ISM in this galaxy (traced by the [CII] line observed in Band 9), at 0.32'' resolution and with a 50 km s^{-1} bandwidth, sufficient to resolve the line. The ALMA data will be complemented by deep HST spatially-resolved CANDELS ACS+WFC3 imaging and 3D-HST WFC3 grism spectroscopy with similar spatial resolution already in hand, and an upcoming LBT high-resolution rest-frame optical spectrum. The proposed observations will provide the first-ever detailed study of the physics and the kinematics of the star-forming ISM in an extremely low-metallicity, low-mass galaxy at $z \simeq 2$, an epoch when the Universe was

Through the magnifying glass: a unique view of the low-metallicity ISM at high redshift¹

Introduction: a gravitationally-lensed, metal-poor dwarf galaxy at the peak of cosmic star formation
Extensive look-back galaxy surveys have revealed that the star formation rate density of the Universe crested at redshifts between 1.5 and 2.5 (e.g. Hopkins & Beacom 2006), and that about half of the stellar mass of the present Universe was already in place at $z \simeq 1.5$. It has become clear that characterizing star-forming galaxies at this key epoch of galaxy build-up is a crucial step towards understanding the evolution of galaxies. The luminosity and stellar mass functions of galaxies at $z \simeq 2$ (Marchesini et al. 2012, Reddy & Steidel 2009, Lee et al. 2012) indicate that up to 50% of all star formation occurring at this epoch takes place in low-mass galaxies ($M_* < 10^9 M_\odot$). Yet, there is basically no spatially-resolved information on the various ISM phases, and the star formation process and locations in such low-mass galaxies at $z \simeq 2$. This makes our understanding of a large part of the star formation occurring at $z \simeq 2$ still very limited to date.

Extremely fortuitously, a low-mass, low-metallicity, star-forming galaxy at $z = 1.847$ in the UDS field (SL2SJ02176-0513; at R.A.= 02^h17^m37^s.237, Dec.= −05°13'29".78) happens to be outstandingly gravitationally lensed by a foreground elliptical galaxy at $z = 0.6459$ (Cabanac et al. 2007, Tu et al. 2009) into three bright images that form a striking tangential arc and a counter image (Fig.1). This is an exceptionally rare gravitational lens system (modeled in detail by Tu et al. 2009, Cooray et al. 2011 and our team [Fig.1c]) which, with a total magnification $\mu_{\text{tot}} \simeq 34$ (as discussed in Fig.1), offers a unique view of the background source, and stretches the images of this dwarf galaxy (which, unlensed, would be barely resolved in high-resolution HST imaging) into an arc spanning over 2.5 arcsec. The counter image is marginally resolved in the HST/ACS images, which allows us to place an upper limit on the effective radius of this galaxy of 350 pc. In the arc, multiple images of two individual star-forming clumps can be separated. The spectrum of the SL2SJ02176-0513 arc was observed with the HST/WFC3 G141 grism as part of the 3D-HST survey (P.I. van Dokkum; Brammer et al. 2012a,b), and it shows very strong [OIII], H β , H γ , H δ and [NeIII] emission (Fig.2), which provide unprecedented diagnostics of the ionized ISM in this galaxy. The Balmer line ratios indicate low dust attenuation ($A_V \simeq 0.2$); moreover, the emission line morphology is similar to the UV continuum morphology (traced by the ACS F606W band), which indicates that extinction affects the UV continuum and lines similarly. In Brammer et al. (2012b) we perform a detailed analysis of these emission lines combined with ACS and WFC3 imaging and find that this galaxy has a (de-magnified) stellar mass $\simeq 10^8 M_\odot$, star formation rate $\simeq 10 M_\odot \text{ yr}^{-1}$ and very low gas-phase metallicity, $12 + \log(\text{O/H}) = 7.5$ (i.e. < 10% of solar metallicity). This stellar mass and SFR imply an exceptionally short stellar mass doubling timescale (< 10 Myr), which means that we must be witnessing this galaxy during a phase of strong growth and feedback. In effect, thanks to the large magnification factor, this source appears to the observer as a low-metallicity, $\simeq 400 M_\odot \text{ yr}^{-1}$ starburst.

While this high magnification lensing system is rare, the type of galaxy it has brought into prominent view is not rare at all. Indeed, an important population of low-mass galaxies at $z \simeq 2$ with physical properties similar to the SL2SJ02176-0513 dwarf has been recently uncovered using deep HST/WFC3 observations, and the number of these galaxies in the young Universe may be even higher than initially suggested (van der Wel et al. 2011, Maseda et al. 2013). However, little is known about the details of the star formation process, ISM properties and gas motions for these low-mass galaxies due to their small sizes. **The enormous gravitational lensing magnification of SL2SJ02176-0513 provides a unique opportunity to spatially resolve the star formation and the ISM in an extremely low-mass, starbursting dwarf galaxy at $z \simeq 2$, which would be impossible for non-lensed systems.** This source represents a truly peerless case of a high-redshift dwarf galaxy magnified 34 times and resolved to physical scales ~ 150 pc, thus providing an unpaired window into the low-metallicity ISM of low-mass galaxies at $z \simeq 2$.

This proposal: We propose to take advantage of the unique magnification of SL2SJ02176-0513, combined with the unmatched resolution and sensitivity of ALMA, to obtain a detailed map of the spatial distribution and kinematics of the star-forming ISM in this galaxy (traced by the [CII] line observed in Band 9), at 0.32" resolution and with a 50 km s $^{-1}$ bandwidth, sufficient to resolve the line. The ALMA data will be complemented by deep HST spatially-resolved CANDELS ACS+WFC3 imaging and 3D-HST WFC3 grism spectroscopy with similar spatial resolution already in hand, and an upcoming LBT high-resolution rest-frame optical spectrum. The proposed observations will provide the first-ever detailed study of the physics and the kinematics of the star-forming ISM in an extremely low-metallicity, low-mass galaxy at $z \simeq 2$, an epoch when the Universe was



Fig. 1: (a) **HST 5''x5'' three-colour image of the SL2SJ02176-0513 gravitational lens system.** (b) Same image, with the foreground elliptical lens removed. Our target is the $z = 1.847$ galaxy lensed into the striking arc, showing the distribution of the rest-frame UV/optical light. Several lensed images of two main resolved star-forming clumps in this galaxy can be observed ('a' and 'b' labelled in the arc and in the counter image). The conjugate images of an additional lensed object, 'x', at $z = 2.29$, are also indicated (Brammer et al. 2012b). We do not expect emission from the lens galaxy (an elliptical) to contaminate our observations of the arc. In the unlikely case there is some emission from the lens, the spatial resolution of our observations (0.32") will allow us to cleanly subtract it similarly to what was done in the HST images. (c) **Our best-fit gravitational lens model** using the method by coe & der (1996), which produces an analytical lens model that follows the non-spherical underlying mass distribution of the lens. The model with an isothermal radial slope $\alpha = -1$ for the density profile is consistent with independent modelling by Tu et al. (2009) fits the image positions a_1, a_2, a_3 and a_x , and yields the individual magnification factors indicated in red; the total magnification for this model is $\mu_{\text{tot}} = 33.7$. We note that while this model provides an excellent fit to the image positions and is consistent with other modelling efforts, the density slope α is less well constrained. We explore a range of realistic values for α between -0.8 and -1.2 , for which the predicted source positions remain well within the errors on the observed positions; these slope values imply total magnifications μ_{tot} between 24.5 and 55.5. **Our proposed [CII] observations will provide a dust-unbiased measure of the flux ratios between the different source images that we will input into our lens modelling to constrain simultaneously the shape and radial slope of the density profile, and thus the total magnification** (van de Ven et al. 2010).

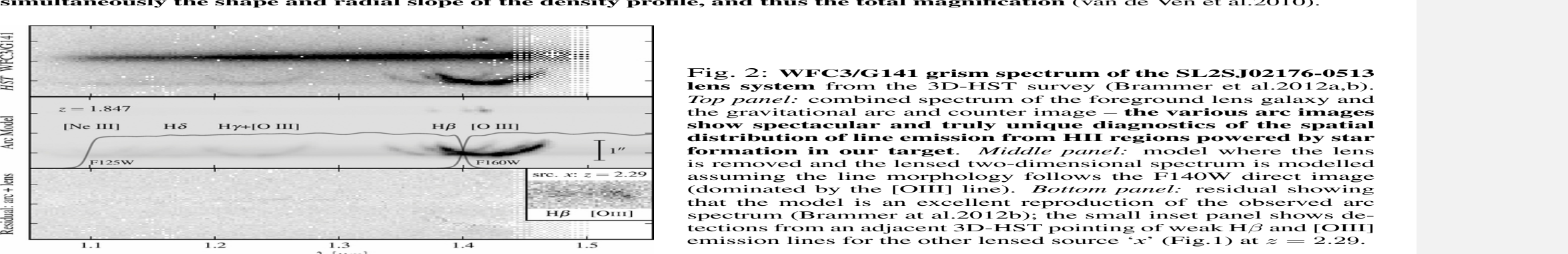


Fig. 2: **WFC3/G141 grism spectrum of the SL2SJ02176-0513 lens system** (from the 3D-HST survey (Brammer et al. 2012a,b)). **Top panel:** combined spectrum of the foreground lens galaxy and the gravitational arc and counter image – the various arc images show spectacular and truly unique diagnostics of the spatial distribution of line emission from HII regions powered by star formation in our target. **Middle panel:** model where the lens is removed and the lensed two-dimensional spectrum is modelled assuming the line morphology follows the F140W direct image (dominated by the [OIII] line). **Bottom panel:** residual showing that the model is an excellent reproduction of the observed arc spectrum. Brammer et al. (2012b) the small inset shows detections from the adjacent 3D-HST grism of weak H β and [OIII] emission lines for the other lensed source 'x' (Fig.1) at $z = 2.29$.

¹The only other known strongly lensed high-redshift dwarf galaxy (van der Wel et al. 2013) is not a suitable target because (i) the lensing configuration is not as ideal (less gain in spatial resolution and challenging lens subtraction) and (ii) the WFC3 grism is highly contaminated by the lens, so we do not have the same exquisitely detailed view of the star formation activity, dust attenuation and metallicity.

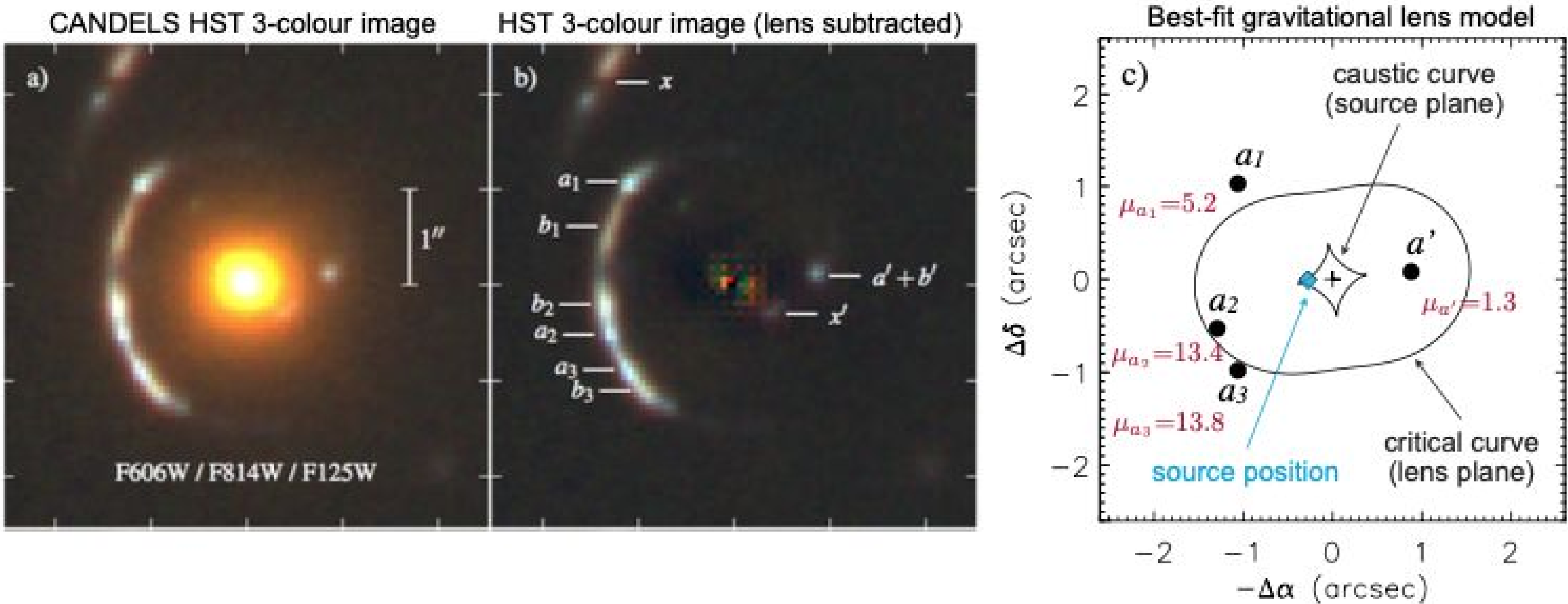


Fig. 1: (a) **HST $5'' \times 5''$ three-colour image of the SL2SJ02176-0513 gravitational lens system.** (b) Same image, with the foreground elliptical lens removed. Our target is the $z = 1.847$ galaxy lensed into the striking arc, showing the distribution of the rest-frame UV/optical light. Several lensed images of two main resolved star-forming clumps in this galaxy can be observed (' a ' and ' b ' labelled in the arc and in the counter image). The conjugate images of an additional lensed object, ' x ', at $z = 2.29$, are also indicated (Brammer et al. 2012b). We do not expect emission from the lens galaxy (an elliptical) to contaminate our observations of the arc. In the unlikely case there is some emission from the lens, the spatial resolution of our observations ($0.32''$) will allow us to cleanly subtract it similarly to what was done in the HST images. (c) **Our best-fit gravitational lens model** using the method by co-I van de Ven et al. (2010) which produces an analytical lens model that allows for a non-spherical underlying mass distribution of the lens. The model with an isothermal radial slope $\alpha = -1$ for the density profile (consistent with independent modelling by Tu et al. 2009) fits the image positions a_1 , a_2 , a_3 and a' , and yields the individual magnification factors indicated in red; the total magnification for this model is $\mu_{\text{tot}} = 33.7$. We note that while this model provides an excellent fit to the image positions and is consistent with other modelling efforts, the density slope α is less well constrained. We explore a range of realistic values for α between -0.8 and -1.2 , for which the predicted source positions remain well within the errors on the observed positions; these slope values imply total magnifications μ_{tot} between 24.5 and 55.5 . **Our proposed [CII] observations will provide a dust-unbiased measure of the flux ratios between the different source images that we will input into our lens modelling to constrain simultaneously the shape and radial slope of the density profile, and thus the total magnification** (van de Ven et al. 2010).

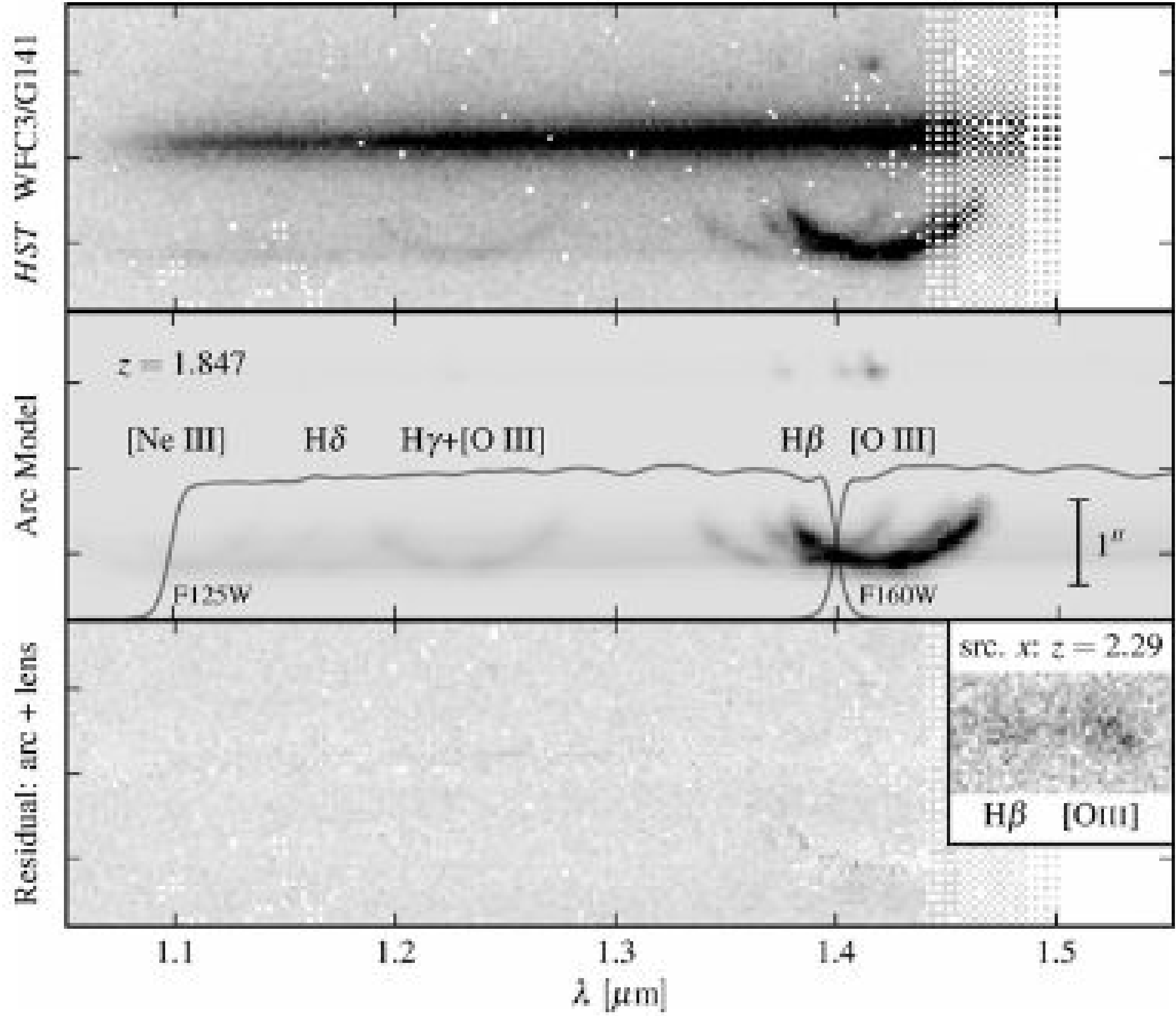


Fig. 2: WFC3/G141 grism spectrum of the SL2SJ02176-0513 lens system from the 3D-HST survey (Brammer et al. 2012a,b). **Top panel:** combined spectrum of the foreground lens galaxy and the gravitational arc and counter image – **the various arc images show spectacular and truly unique diagnostics of the spatial distribution of line emission from HII regions powered by star formation in our target.** **Middle panel:** model where the lens is removed and the lensed two-dimensional spectrum is modelled assuming the line morphology follows the F140W direct image (dominated by the [OIII] line). **Bottom panel:** residual showing that the model is an excellent reproduction of the observed arc spectrum (Brammer et al. 2012b); the small inset panel shows detections from an adjacent 3D-HST pointing of weak H β and [OIII] emission lines for the other lensed source ‘x’ (Fig.1) at $z = 2.29$.

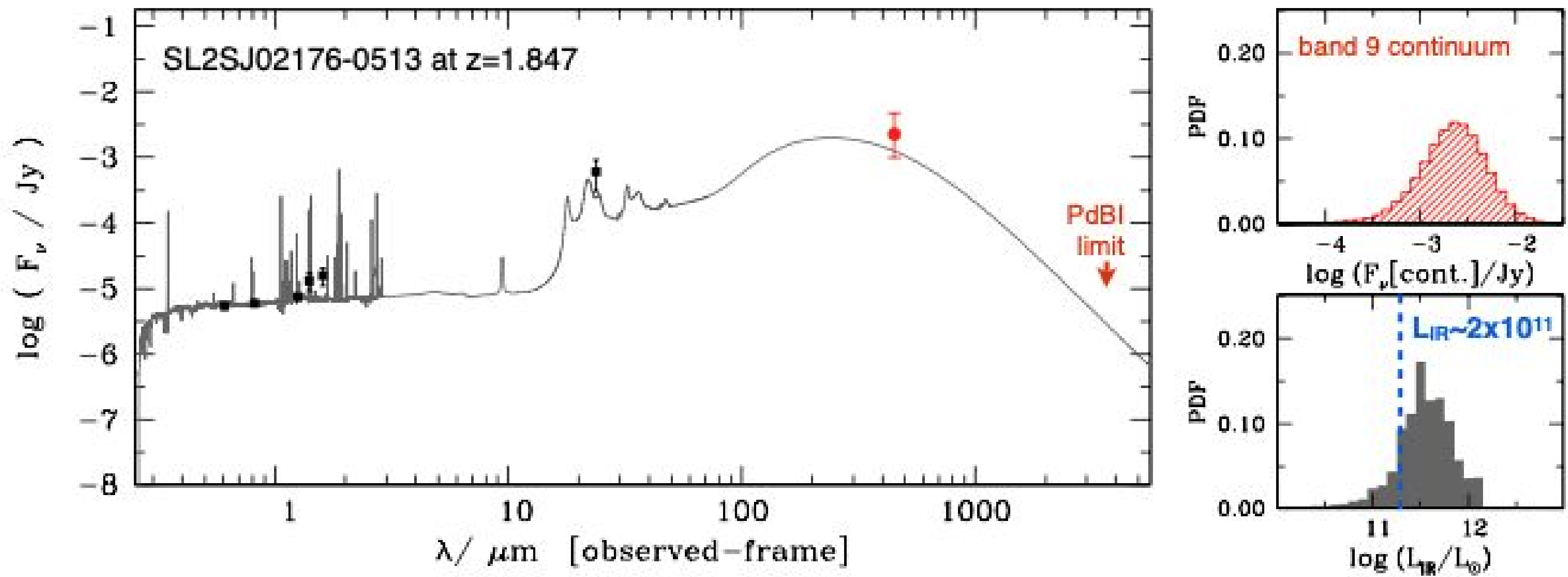


Fig. 3: Fit to the (magnified) spectral energy distribution (SED) of our lensed low-mass galaxy. *Black points:* observed fluxes (including the marginal MIPS 24- μm detection); *red point:* predicted Band-9 continuum flux; *red arrow:* continuum sensitivity reached by our PdBI observations at $\simeq 80$ GHz (23 μJy). We include the emission line flux in the broad bands (using the models by Pacifici et al. 2012) and compute the infrared SED consistently with the inferred dust attenuation of the continuum + lines in terms of energy balance using the MAGPHYS model (da Cunha et al. 2008). We derive Bayesian likelihood distributions for the total infrared luminosity L_{IR} and the 158 μm continuum – we incorporate our uncertainties due to the lack of data in the far-IR by marginalizing over a large library of dust emission models with different PAHs contributions and dust temperatures (da Cunha et al. 2013). This allows us to derive robust, physically-consistent estimates for the expected total dust luminosity (and hence [CII] luminosity) and Band-9 continuum flux for our galaxy. We take a (conservative) estimate of $L_{\text{IR}} = 2 \times 10^{11} L_\odot$ (not corrected for lensing).

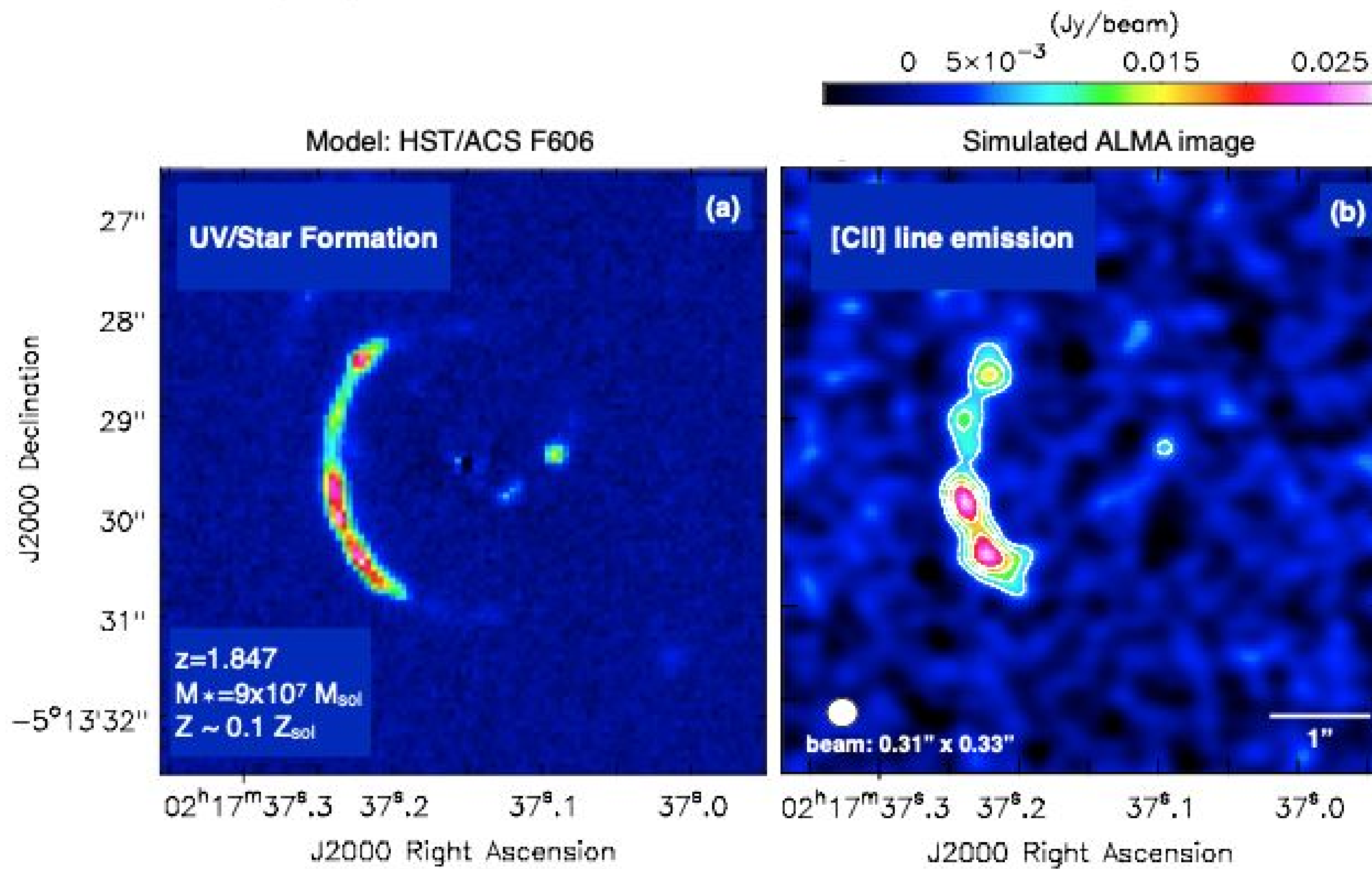


Fig. 4: CASA simulated ALMA [CII] line map of SL2SJ02176-0513 at $\sim 0.3''$ resolution (Cycle 3 C36-2 antenna configuration), 111 MHz bandwidth at 667.58 GHz, 2 mJy/beam rms (total 44 minutes on-source). (a) Input model: HST/ACS F606W image at 0.2'' resolution, mapping the rest-frame UV emission; (b) Simulated [CII] map (including noise); the contours show the 3-, 5-, 7- and 9- σ levels. This shows that the requested sensitivity of 2 mJy/beam is needed to detect the faintest regions of the arc (if the [CII] emission is distributed in the same way as the star formation rate).

Technical Justification

2015.1.00050.S

SG : 1 of 1 SL2SJ02176-0513 Band 9

[CII] in the low-metallicity dwarf galaxy at z=1.84691

Science Goal Parameters

Ang.Res.	LAS	Requested RMS	RMS Bandwidth	Rep.Freq.	Cont. RMS	Cont. Bandwidth	Poln.Prod.	Non-standard mode
0.32"	2.5"	2 mJy, 53.6 mK	49.847 km/s, 111 MHz	667.578849 GHz	242.7 μJy, 6.5 mK	7.500 GHz	XX,YY	Yes

Use of 12m Array (36 antennas)

t_total (all configs)	t_science (extended)	t_total(compact)	Imaged area	#12m pointing	12m Mosaic spacing	HPBW	t_per_point	Data Vol	Data Rate
1.7 h	0.8 h	0.0 s	2.9 "	1	offset	8.7 "	2782.0 s	18.5 GB	3.1 MB/s

Use of ACA 7m Array (10 antennas) and TP Array

t_total(ACA)	t_total(7m)	t_total(TP)	Imaged area	#7m pointing	7m Mosaic spacing	HPBW	t_per_point	Data Vol	Data Rate

1 Target

No.	Target	Ra,Dec(J2000)	V,def,frame --OR--z
1	1-SL2SJ02176-05...	02:17:37, -05:13:29	194487.95 km/s, lsrk, RADIO

Expected Source Properties

	Peak Flux	SNR	Pol.	Pol. SNR	Linewidth	RMS (over 1/3 linewidth)	linewidth / bandwidth used for sensitivity
Line	28.00 mJy	12.6	0.0%	0.0	120 km/s	2.23 mJy, 59.7 mK	2.41
Continuum	15.00 uJy	0.1	0.0%	0.0	0 km/s		

Dynamic range (cont flux/line rms): 0.0

1 Tuning

Tuning	Target	Rep. Freq. Sky GHz	RMS (Rep. Freq.)	RMS Achieved
1	1	667.578849	1.99 mJy, 53.5 mK	1.95 mJy - 2.15 mJy

Spectral Setup : Spectral Line

BB	Center Freq Rest GHz	spw name	Eff #Ch p.p.	Bandwidth	Resolution	Vel. Bandwidth	Vel. Res.	Res. El. per FWHM
1	1900.536900	CII 2P3/2-2P1/2 [spw1]	3840	1875.00 MHz	3904.297 kHz	842.1 km/s	1.753 km/s	68
2	1906.006245	Manual Window [spw2]	3840	1875.00 MHz	3904.297 kHz	839.7 km/s	1.748 km/s	69
3	1850.135636	Manual Window [spw3]	3840	1875.00 MHz	3904.297 kHz	865.0 km/s	1.801 km/s	67
4	1844.797680	Manual Window [spw4]	3840	1875.00 MHz	3904.297 kHz	867.5 km/s	1.806 km/s	66

Justification for requested RMS and resulting S/N (and for spectral lines the bandwidth selected) for the sensitivity calculation.

Band Choice: We propose to observe the [CII] line emission (the brightest diagnostic of the star-forming ISM) at rest-frame 1900.54 GHz, so observed at 667.58 GHz (Band 9) for the redshift of our source, $z=1.84691$. Band 9 also provides ideal spatial resolution.

Bandwidth: Our high spectral resolution LBT/LUCI follow-up of 3D-HST low-mass dwarf starburst galaxies (Maseda+2013) obtains typical optical line widths of 120 km/s. Assuming that the [CII] line from SL2SJ02176-0513 has a similar width, our kinematic study requires a minimum velocity resolution of 50 km/s, which corresponds to a bandwidth of 111 MHz at 667.58 GHz.

Requested sensitivity: We predict the total infrared dust luminosity of our source by performing spectral energy distribution modelling of the available observations as shown in Fig.3. The resulting likelihood distribution is relatively broad since we lack infrared observations for our galaxy beyond 24 microns; therefore, we assume a conservative total infrared luminosity of $L_{\text{IR}} \sim 2 \times 10^{11} \text{ L}_{\odot}$ (including magnification), which is about 1 sigma lower than the median of the L_{IR} likelihood distribution. We assume [CII]-to-infrared luminosity ratio of 1.5% - consistent with observations of local low-metallicity dwarf galaxies (Madden+1997), and predict a (magnified) [CII] line luminosity of $3 \times 10^9 \text{ L}_{\odot}$. This implies a velocity-integrated flux of 21.8 Jy km/s. Assuming a line FWHM of 120 km/s (consistent with LBT/LUCI measurements), we predict a total [CII] flux density of 181 mJy for our source. To achieve an average 9-sigma detection per beam over ~ 10 beams, we require a sensitivity of 2 mJy/beam, which, with the requested bandwidth of 111 MHz, would be reached in 44 minutes on source (1.7 hours in total including current Cycle 3 calibration and overheads) assuming 36 antennas in the C36-2 configuration. The simulated [CII] image in Fig.4, resulting from the proposed set-up, shows that this sensitivity is needed to detect the [CII] emission at significant levels (at least 3-sigma) along the whole gravitational arc.

Our SED fitting predicts a total continuum flux at rest-frame 158um of ~ 2.2 mJy (Fig.3). Assuming 43 mins integration time in the C36-2 configuration required for our line observations and an aggregate 7.5 GHz band width, we find that it is unlikely that the dust continuum will be detected with the predicted continuum sensitivity of 0.24 mJy/beam. However, our observations will allow us to gain in continuum sensitivity by stacking the flux on the three different images of the galaxy along the gravitational arc. This will allow us to set a robust upper limit on the rest-frame 158um flux and on the total infrared luminosity of the galaxy. Compared with the measured [CII], this will allow us to place a lower limit on [CII]-to-infrared luminosity ratio - a diagnostic tool of the radiation field of the ISM (Stacey+2010).

Justification of the chosen angular resolution and largest angular scale for the source(s) in this Science Goal.

Since we aim at spatially resolving the [CII] emission with a comparable resolution to that of the HST continuum and emission line images, we require an intermediate resolution of 0.32 arcsec (achievable with the C36-2 Cycle 3 antenna configuration; the C36-3 configuration would also be acceptable); no ACA is required since the arc does not show extended emission at scales larger than 2.5 arcsec. This resolution corresponds to a minimum physical scale of ~150 parsecs in the lensed arc, providing a detailed view of the cool ISM at $z \sim 2$. Simulations of our proposed observations with CASA show that the requested configuration is optimal to obtain a high S/N [CII] line map that can be directly compared with our HST data (Fig.4).

Justification of the correlator set-up with particular reference to the number of spectral resolution elements per line width.

Four 1875 MHz-wide spectral windows: spw1 centered at the [CII] line (667.58 GHz); spw2 in the same sideband, at 669.5 GHz; spw3 and spw4 in the opposite sideband, at 649.87 and 648 GHz. These were selected to cover our target line and avoid strong atmospheric absorption features. We request a resolution of 3.904 MHz in each spectral window, sufficient to sample the line with 68 spectral resolution elements, while keeping the data rate low.

Successful ALMA Proposal

A complete census of dust in sub-millimetre galaxies

ABSTRACT

The ALMA Cycle 0 follow-up of sub-mm sources in the ECDF-South at 345 GHz (Band7) has allowed us to pin-point the locations of sub-millimeter galaxies (SMGs), and build the most statistically reliable sample of SMGs to date, ALESS, which contains 99 SMGs with a median redshift of 2.7.

We propose to complete the characterization of the IR/sub-mm SEDs of the ALESS SMGs by obtaining their total continuum fluxes at 679GHz (Band 9) and 145GHz (Band 4). These observations, combined with existing continuum fluxes in Band 7, are crucial to fully characterize the amount and physical properties of dust in our SMGs. By measuring near the peak of the dust emission (Band 9), and in the Rayleigh-Jeans regime (Band 4), we will constrain the dust masses of our galaxies at least 5 times more precisely than possible with current observations. With these properties in hand, we will test models of dust formation and growth at high- z , investigate the properties of dust grains and dust heating processes in SMGs, and derive gas masses in order to establish the star formation efficiency and gas depletion timescale in high-redshift SMGs, and eventually gain insights into their mode of star formation.

Scientific Justification

A complete census of dust in sub-millimeter galaxies

Introduction

The dustiest galaxies in the Universe. Sub-millimeter galaxies (SMGs) are the most dusty galaxies in the high-redshift Universe ($z \gtrsim 2$), with large infrared (IR) luminosities powered by intense star formation activity. Although these galaxies are relatively rare (e.g. Weiss et al. 2009), they are a crucial population to understand the broad picture of galaxy evolution. SMGs have high star formation rates (SFR $> 100 M_{\odot}/\text{yr}$), contributing up to half of the SFR density at $z > 1$, and they are possibly the progenitors of the most massive galaxies in the local Universe (e.g. Blain et al. 2002, Casey et al. 2014, Simpson et al. 2014). Their large amounts of dust make them ideal objects to study how dust forms in the high- z interstellar medium (ISM), and to study the interplay between star formation activity, gas and dust.

Over recent years, there has been much debate on the origin of the large dust masses of SMGs (typically $> 10^8 M_{\odot}$, i.e. a few percent of their stellar mass), that were inferred (mostly) from single-dish sub-millimeter observations and/or for biased samples of SMGs (e.g. Michalowski 2015, Rowlands et al. 2014). Studies of high-redshift SMGs are finding that the build-up of large dust masses in these galaxies in timescales $\sim 0.5 - 2$ Gyr is extremely difficult to explain by dust production and growth models (e.g. Morgan & Edmunds 2003, Dwek et al. 2007) using stellar sources alone (AGB stars and supernovae), and explanations such as ISM dust growth and/or non-standard IMFs are required (the so-called ‘SMG dust budget crisis’; e.g. Rowlands et al. 2014). More precise dust mass constraints for unbiased samples of SMGs are needed to further investigate this issue.

Another matter of debate in the community is what drives the large SFRs of SMGs: whether it is a mode of enhanced star formation efficiency driven by major mergers (e.g. Hayward et al. 2011), or a more modest star formation efficiency driven by secular evolution in large disks with high gas fractions (e.g. Davé et al. 2011), or a mix of both. A step to disentangle these two evolutionary modes is to compare the observed SFRs with the mass of gas available to form stars in SMGs which, until we have CO observations for large samples, can be inferred from the dust mass (assuming $M_{\text{gas}}/M_{\text{dust}}$; Scoville et al. 2014, Groves et al. 2015).

ALESS: an unbiased sample of SMGs. The APEX LABOCA 870- μm survey of the Extended *Chandra* Deep Field South, LESS, is the largest and deepest contiguous survey ever performed at that wavelength, and identified 126 sub-millimeter sources with 870- μm fluxes above 4 mJy (Weiss et al. 2009). 122 of the LESS sources were followed-up at the same wavelength, with unprecedentedly high sensitivity and spatial resolution enabled by ALMA in the Cycle 0 program ALESS (snapshot observations in Band 7; Karim et al. 2013, Hodge et al. 2013). The high resolution enabled by ALMA allowed for a de-blending of multiple sources that were previously identified as a single source due to the large beam of single-dish observations, and to pin-point the location of the detected SMGs to within 0.3” (Hodge et al. 2013). These observations yield a sample of 99 robustly identified ALESS SMGs. *This is the most statistically reliable survey of SMGs, which allows for a complete and unbiased multi-wavelength study of the properties of this important galaxy population.* ALESS is the ideal sample to study, for the first time, the star formation properties and dust content of sub-millimeter galaxies in an unbiased way. In Fig.1, we plot the distribution of redshifts, stellar masses, star formation rates and total dust luminosities of the ALESS sources obtained from modelling their UV-to-radio spectral energy distributions (Simpson et al. 2014, da Cunha et al. 2015).

Obtaining the precise locations and 870- μm fluxes of the ALESS SMGs allowed us to extract far-IR fluxes from *Herschel*/SPIRE maps using a de-blending algorithm to beat the poor resolution of the *Herschel* observations (Swinbank et al. 2014). Far-IR observations sample the dust emission peak and constrain the total IR luminosity (i.e. SFR), dust temperature and dust mass. However, the *Herschel* fluxes have large uncertainties (compared to ALMA), and 34 (i.e. one third) of the ALESS SMGs do not have a 3 σ SPIRE counterpart. Moreover, the current lack of observations at wavelengths longer than 870 μm means that we do not have a good handle on the Rayleigh-Jeans slope of the dust emission, which is crucial to estimate dust mass. For the sources with no *Herschel* fluxes (and those with large flux errors), we find in da Cunha et al. 2015 that the dust luminosity, mass and temperature are very hard to constrain precisely (median error bars 0.5 dex, 0.8 dex, and 18 K, respectively), and we do not even attempt to constrain the dust emissivity index due to the current lack of long wavelength observations to constrain the Rayleigh-Jeans slope.

This proposal. We propose to complete the characterization of the infrared/sub-millimeter spectral energy distributions of the ALESS SMGs by obtaining their total continuum fluxes at 679 GHz (ALMA Band 9) and at 145 GHz (ALMA Band 4). These observations will complement our current precise measurements of the total flux at 345 GHz obtained with Band 7 in Cycle 0, and will allow us to fully characterize the amount and physical properties of dust in our unbiased, well-defined sample of SMGs.

Science goal

The main goal of our proposal is **to obtain the complete dust SEDs of our unbiased and well characterized sample of SMGs**, including one flux measurement near the peak of the dust emission (with ALMA Band 9) and one flux measurement in the Rayleigh-Jeans tail of the dust emission (with Band 4).

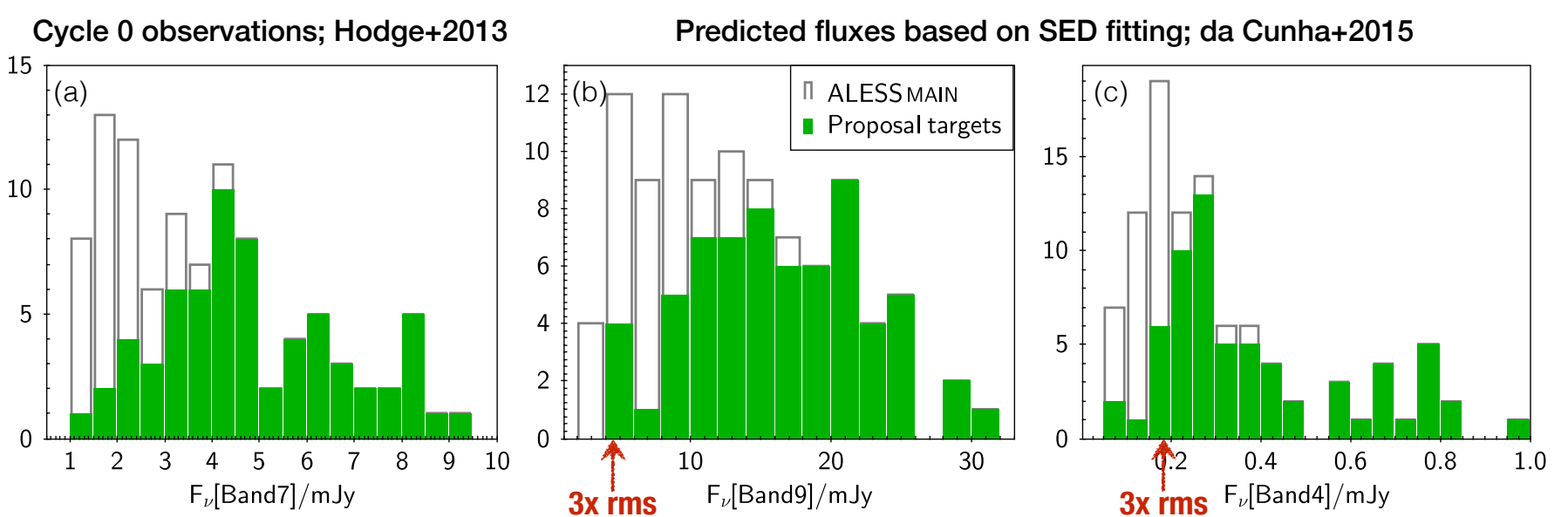
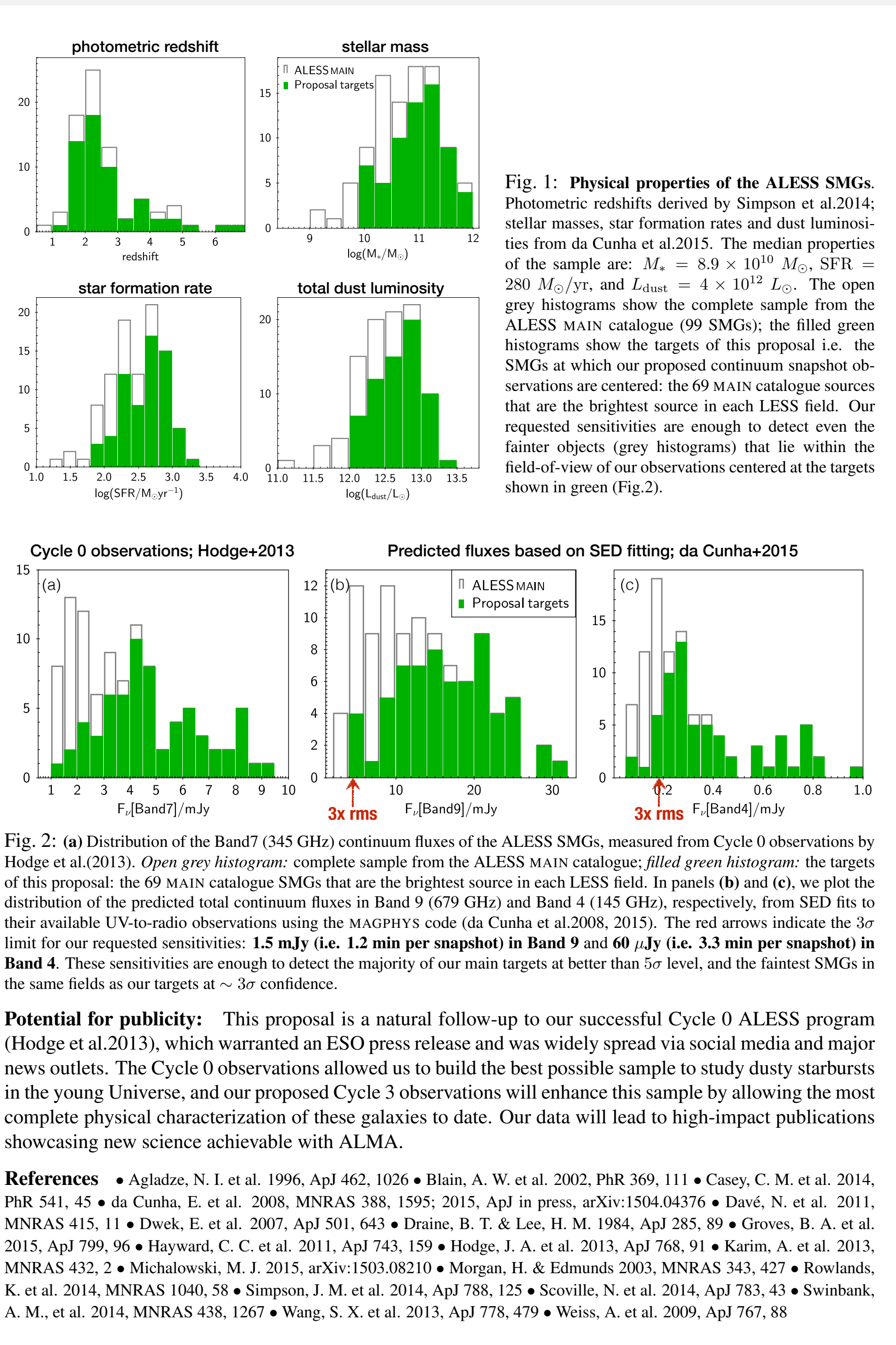
The mass of dust in a galaxy with equilibrium temperature T_{dust} is given by $M_{\text{dust}} \propto L_{\text{dust}}/T_{\text{dust}}^{4+\beta}$, where L_{dust} is the total dust luminosity, and β is the dust emissivity index, which defines the emissivity of the dust grains as a function of frequency, and depends on the properties of the dust grains (chemical composition, size, shape). Theoretical models and laboratory studies predict a range of values for this parameter, from $\beta \simeq 1$ for small carbonaceous grains, and $\beta \simeq 2$ or higher for amorphous silicate grains (e.g. Draine & Lee 1984, Agladze et al. 1996), with some dependence on temperature. In Fig.3, we plot model dust SEDs of galaxies at $z = 2.7$ (the median redshift of our sample), with varying values of T_{dust} and β . These plots show that the shape of the dust emission is a strong function of these parameters in different wavelength ranges, and therefore observables sampling the full dust SED are needed to constrain effectively T_{dust} , β , (also L_{dust}) and hence get precise constraints on M_{dust} .

Constraining the **peak of the dust emission with Band 9** is crucial to obtain precise measurements of L_{dust} (which is very close to the bolometric luminosity for SMGs, and will be used to get tighter constraints on the SFR), and of the dust temperature, which will provide insight into the dust heating conditions in SMGs. A longer-wavelength **measurement in the Rayleigh-Jeans regime with Band 4** (combined with available Band 7 observations) will allow us to measure the slope of the Rayleigh-Jeans tail of the SED, which depends directly on the dust emissivity index β . This will allow us to obtain robust constraints on M_{dust} , and to understand the properties of dust at high redshift, by comparing our derived values of β with predictions from theoretical dust grain models. **Fig.4 shows that our proposed observations in Band 9, Band 7 (already in hand) and Band 4, are essential to obtain the best possible constraints of the dust mass of our galaxies (at better than 0.2 dex, i.e. at least 5 times more precise than current estimates), because they break the degeneracy between T_{dust} and β .**

Science questions that we will address with our proposed observations:

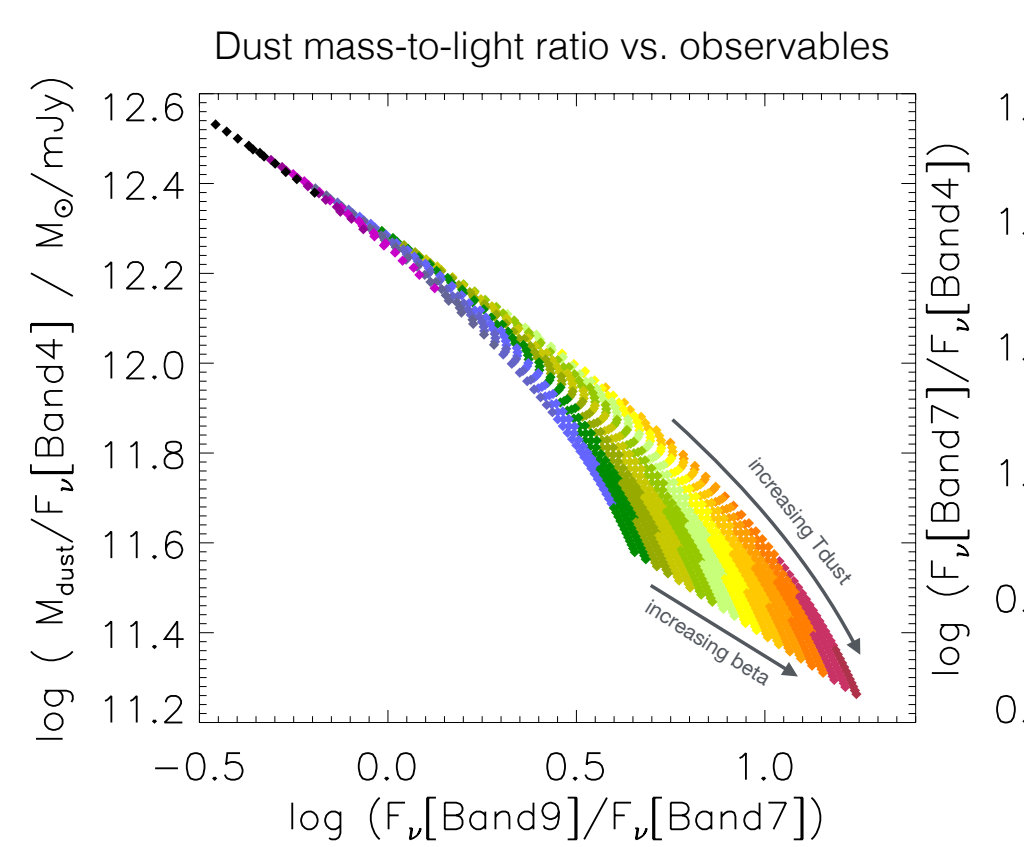
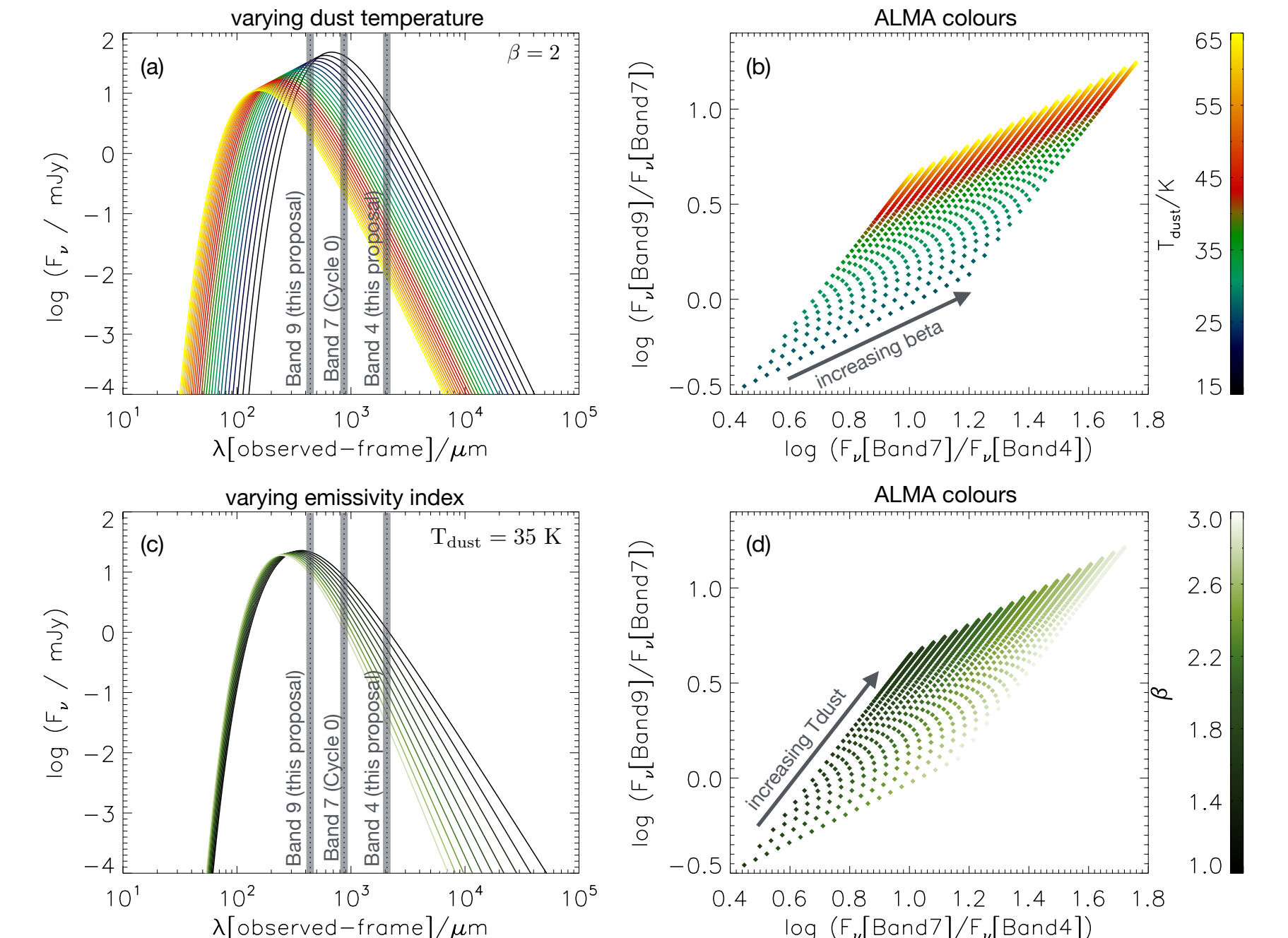
- **Mass of dust in SMGs:** What is the dust mass distribution of our unbiased SMG sample? Can the dust masses be explained using current dust formation and growth models?
- **Properties of the dust grains:** What is the emissivity index of the dust in SMGs? What type of dust grains do we observe in the ISM of high-redshift starbursts, i.e. are the β values more consistent with carbonaceous or silicate grains? Are the dust properties the same across all SMGs, or do we see variation with galaxy properties (such as star formation activity, temperature)? Do X-ray AGN (identified and characterized in our sample by Wang et al. 2013) have any impact in the dust properties?
- **Temperature of dust in SMGs:** Is the dust hot, consistent with compact starbursts, or cooler, consistent with more extended distributions of stars and dust?
- **Gas masses derived from dust masses:** What are the gas fractions of our SMGs? What is the gas depletion timescale i.e. the SF efficiency? We will interpret the results in the context of what galaxy evolution models predict for starburst-driven mergers vs. gas-rich, secularly-evolving galaxies.

We estimate the expected total Band 9 and 4 continuum fluxes (Fig.2) using our fits to the full available UV-to-radio SED for each ALESS SMG (da Cunha et al. 2015). We propose to take snapshot observations centered at each of the brightest ALESS sources in each LESS field. Our (unresolved) continuum observations will reach a sensitivity of **1.5 mJy in Band 9 in 1.2 min, and 0.060 mJy in Band 4 in 3.3 min per snapshot (i.e. a total time on-source of 1.4 h in Band 9 and 3.8 h in Band 4 for 69 snapshots)**. This will allow us to detect the majority of our main targets (green in Fig.2) at better than 5 σ level, and the faintest SMGs in the same fields as our targets (that will fall in the FOV) at $\sim 3\sigma$ confidence (grey in Fig.2).



Potential for publicity: This proposal is a natural follow-up to our successful Cycle 0 ALESS program (Hodge et al. 2013), which warranted an ESO press release and was widely spread via social media and major news outlets. The Cycle 0 observations allowed us to build the best possible sample to study dusty starbursts in the young Universe, and our proposed Cycle 3 observations will enhance this sample by allowing the most complete physical characterization of these galaxies to date. Our data will lead to high-impact publications showcasing new science achievable with ALMA.

References • Agladze, N. I. et al. 1996, ApJ 462, 1026 • Blain, A. W. et al. 2002, PhR 369, 111 • Casey, C. M. et al. 2014, PhR 541, 45 • da Cunha, E. et al. 2008, MNRAS 388, 1595; 2015, ApJ in press, arXiv:1504.04376 • Davé, N. et al. 2011, MNRAS 415, 11 • Dwek, E. et al. 2007, ApJ 501, 643 • Draine, B. T. & Lee, H. M. 1984, ApJ 285, 89 • Groves, B. A. et al. 2015, ApJ 799, 96 • Hayward, C. C. et al. 2011, ApJ 743, 159 • Hodge, J. A. et al. 2013, ApJ 768, 91 • Karim, A. et al. 2013, MNRAS 432, 2 • Michalowski, M. J. 2015, arXiv:1503.08210 • Morgan, H. & Edmunds 2003, MNRAS 343, 427 • Rowlands, K. et al. 2014, MNRAS 1040, 58 • Simpson, J. M. et al. 2014, ApJ 788, 125 • Scoville, N. et al. 2014, ApJ 783, 43 • Swinbank, A. M., et al. 2014, MNRAS 438, 1267 • Wang, S. X. et al. 2013, ApJ 778, 479 • Weiss, A. et al. 2009, ApJ 767, 88



The dustiest galaxies in the Universe. Sub-millimeter galaxies (SMGs) are the most dusty galaxies in the high-redshift Universe ($z \gtrsim 2$), with large infrared (IR) luminosities powered by intense star formation activity. Although these galaxies are relatively rare (e.g. Weiss et al. 2009), they are a crucial population to understand the broad picture of galaxy evolution. SMGs have high star formation rates ($\text{SFR} > 100 M_{\odot}/\text{yr}$), contributing up to half of the SFR density at $z > 1$, and they are possibly the progenitors of the most massive galaxies in the local Universe (e.g. Blain et al. 2002, Casey et al. 2014, Simpson et al. 2014). Their large amounts of dust make them ideal objects to study how dust forms in the high- z interstellar medium (ISM), and to study the interplay between star formation activity, gas and dust.

Over recent years, there has been much debate on the origin of the large dust masses of SMGs (typically $> 10^8 M_{\odot}$, i.e. a few percent of their stellar mass), that were inferred (mostly) from single-dish sub-millimeter observations and/or for biased samples of SMGs (e.g. Michalowski 2015, Rowlands et al. 2014). Studies of high-redshift SMGs are finding that the build-up of large dust masses in these galaxies in timescales $\sim 0.5 - 2$ Gyr is extremely difficult to explain by dust production and growth models (e.g. Morgan & Edmunds 2003, Dwek et al. 2007) using stellar sources alone (AGB stars and supernovae), and explanations such as ISM dust growth and/or non-standard IMFs are required (the so-called ‘SMG dust budget crisis’; e.g. Rowlands et al. 2014). More precise dust mass constraints for unbiased samples of SMGs are needed to further investigate this issue.

Another matter of debate in the community is what drives the large SFRs of SMGs: whether it is a mode of enhanced star formation efficiency driven by major mergers (e.g. Hayward et al. 2011), or a more modest star formation efficiency driven by secular evolution in large disks with high gas fractions (e.g. Davé et al. 2011), or a mix of both. A step to disentangle these two evolutionary modes is to compare the observed SFRs with the mass of gas available to form stars in SMGs which, until we have CO observations for large samples, can be inferred from the dust mass (assuming $M_{\text{gas}}/M_{\text{dust}}$; Scoville et al. 2014, Groves et al. 2015).

ALESS: an unbiased sample of SMGs. The APEX LABOCA 870- μ m survey of the Extended *Chandra* Deep Field South, LESS, is the largest and deepest contiguous survey ever performed at that wavelength, and identified 126 sub-millimeter sources with 870- μ m fluxes above 4 mJy (Weiss et al. 2009). 122 of the LESS sources were followed-up at the same wavelength, with unprecedentedly high sensitivity and spatial resolution enabled by ALMA in the Cycle 0 program ALESS (snapshot observations in Band 7; Karim et al. 2013, Hodge et al. 2013). The high resolution enabled by ALMA allowed for a de-blending of multiple sources that were previously identified as a single source due to the large beam of single-dish observations, and to pin-point the location of the detected SMGs to within 0.3" (Hodge et al. 2013). These observations yield a sample of 99 robustly identified ALESS SMGs. *This is the most statistically reliable survey of SMGs, which allows for a complete and unbiased multi-wavelength study of the properties of this important galaxy population.* ALESS is the ideal sample to study, for the first time, the star formation properties and dust content of sub-millimeter galaxies in an unbiased way. In Fig.1, we plot the distribution of redshifts, stellar masses, star formation rates and total dust luminosities of the ALESS sources obtained from modelling their UV-to-radio spectral energy distributions (Simpson et al. 2014, da Cunha et al. 2015).

Obtaining the precise locations and 870- μ m fluxes of the ALESS SMGs allowed us to extract far-IR fluxes from *Herschel*/SPIRE maps using a de-blending algorithm to beat the poor resolution of the *Herschel* observations (Swinbank et al. 2014). Far-IR observations sample the dust emission peak and constrain the total IR luminosity (i.e. SFR), dust temperature and dust mass. However, the *Herschel* fluxes have large uncertainties (compared to ALMA), and 34 (i.e. one third) of the ALESS SMGs do not have a 3σ SPIRE counterpart. Moreover, the current lack of observations at wavelengths longer than 870 μ m means that we do not have a good handle on the Raleigh-Jeans slope of the dust emission, which is crucial to estimate dust mass. For the sources with no *Herschel* fluxes (and those with large flux errors), we find in da Cunha et al. 2015 that the dust luminosity, mass and temperature are very hard to constrain precisely (median error bars 0.5 dex, 0.8 dex, and 18 K, respectively), and we do not even attempt to constrain the dust emissivity index due to the current lack of long wavelength observations to constrain the Rayleigh-Jeans slope.

This proposal. We propose to complete the characterization of the infrared/sub-millimeter spectral energy distributions of the ALESS SMGs by obtaining their total continuum fluxes at 679 GHz (ALMA Band 9) and at 145 GHz (ALMA Band 4). These observations will complement our current precise measurements of the total flux at 345 GHz obtained with Band 7 in Cycle 0, and will allow us to fully characterize the amount and physical properties of dust in our unbiased, well-defined sample of SMGs.

Science goal

The main goal of our proposal is **to obtain the complete dust SEDs of our unbiased and well characterized sample of SMGs**, including one flux measurement near the peak of the dust emission (with ALMA Band 9) and one flux measurement in the Rayleigh-Jeans tail of the dust emission (with Band 4).

The mass of dust in a galaxy with equilibrium temperature T_{dust} is given by $M_{\text{dust}} \propto L_{\text{dust}}/T_{\text{dust}}^{4+\beta}$, where L_{dust} is the total dust luminosity, and β is the dust emissivity index, which defines the emissivity of the dust grains as a function of frequency, and depends on the properties of the dust grains (chemical composition, size, shape). Theoretical models and laboratory studies predict a range of values for this parameter, from $\beta \simeq 1$ for small carbonaceous grains, and $\beta \simeq 2$ or higher for amorphous silicate grains (e.g. Draine & Lee 1984, Agladze et al. 1996), with some dependence on temperature. In Fig.3, we plot model dust SEDs of galaxies at $z = 2.7$ (the median redshift of our sample), with varying values of T_{dust} and β . These plots show that the shape of the dust emission is a strong function of these parameters in different wavelength ranges, and therefore observables sampling the full dust SED are needed to constrain effectively T_{dust} , β , (also L_{dust}) and hence get precise constraints on M_{dust} .

Constraining the **peak of the dust emission with Band 9** is crucial to obtain precise measurements of L_{dust} (which is very close to the bolometric luminosity for SMGs, and will be used to get tighter constraints on the SFR), and of the dust temperature, which will provide insight into the dust heating conditions in SMGs. A longer-wavelength **measurement in the Rayleigh-Jeans regime with Band 4** (combined with available Band 7 observations) will allow us to measure the slope of the Rayleigh-Jeans tail of the SED, which depends directly on the dust emissivity index β . This will allow us to obtain robust constraints on M_{dust} , and to understand the properties of dust at high redshift, by comparing our derived values of β with predictions from theoretical dust grain models. **Fig.4 shows that our proposed observations in Band 9, Band 7 (already in hand) and Band 4, are essential to obtain the best possible constraints of the dust mass of our galaxies (at better than 0.2 dex, i.e. at least 5 times more precise than current estimates)**, because they break the degeneracy between T_{dust} and β .

Science questions that we will address with our proposed observations:

- *Mass of dust in SMGs:* What is the dust mass distribution of our unbiased SMG sample? Can the dust masses be explained using current dust formation and growth models?
- *Properties of the dust grains:* What is the emissivity index of the dust in SMGs? What type of dust grains do we observe in the ISM of high-redshift starbursts, i.e. are the β values more consistent with carbonaceous or silicate grains? Are the dust properties the same across all SMGs, or do we see variation with galaxy properties (such as star formation activity, temperature)? Do X-ray AGN (identified and characterized in our sample by Wang et al. 2013) have any impact in the dust properties?
- *Temperature of dust in SMGs:* Is the dust hot, consistent with compact starbursts, or cooler, consistent with more extended distributions of stars and dust?
- *Gas masses derived from dust masses:* What are the gas fractions of our SMGs? What is the gas depletion timescale i.e. the SF efficiency? We will interpret the results in the context of what galaxy evolution models predict for starburst-driven mergers vs. gas-rich, secularly-evolving galaxies.

We estimate the expected total Band 9 and 4 continuum fluxes (Fig.2) using our fits to the full available UV-to-radio SED for each ALESS SMG (da Cunha et al. 2015). We propose to take snapshot observations centered at each of the brightest ALESS sources in each LESS field. Our (unresolved) continuum observations will reach a sensitivity of **1.5 mJy in Band 9 in 1.2 min, and 0.060 mJy in Band 4 in 3.3 min per snapshot (i.e. a total time on-source of 1.4 h in Band 9 and 3.8 h in Band 4 for 69 snapshots)**. This will allow us to detect the majority of our main targets (green in Fig.2) at better than 5σ level, and the faintest SMGs in the same fields as our targets (that will fall in the FOV) at $\sim 3\sigma$ confidence (grey in Fig.2).

This proposal. We propose to complete the characterization of the infrared/sub-millimeter spectral energy distributions of the ALESS SMGs by obtaining their total continuum fluxes at 679 GHz (ALMA Band 9) and at 145 GHz (ALMA Band 4). These observations will complement our current precise measurements of the total flux at 345 GHz obtained with Band 7 in Cycle 0, and will allow us to fully characterize the amount and physical properties of dust in our unbiased, well-defined sample of SMGs.

Science goal

The main goal of our proposal is **to obtain the complete dust SEDs of our unbiased and well characterized sample of SMGs**, including one flux measurement near the peak of the dust emission (with ALMA Band 9) and one flux measurement in the Rayleigh-Jeans tail of the dust emission (with Band 4).

The mass of dust in a galaxy with equilibrium temperature T_{dust} is given by $M_{\text{dust}} \propto L_{\text{dust}}/T_{\text{dust}}^{4+\beta}$, where L_{dust} is the total dust luminosity, and β is the dust emissivity index, which defines the emissivity of the dust grains as a function of frequency, and depends on the properties of the dust grains (chemical composition, size, shape). Theoretical models and laboratory studies predict a range of values for this parameter, from $\beta \simeq 1$ for small carbonaceous grains, and $\beta \simeq 2$ or higher for amorphous silicate grains (e.g. Draine & Lee 1984, Agladze et al. 1996), with some dependence on temperature. In Fig.3, we plot model dust SEDs of galaxies at $z = 2.7$ (the median redshift of our sample), with varying values of T_{dust} and β . These plots show that the shape of the dust emission is a strong function of these parameters in different wavelength ranges, and therefore observables sampling the full dust SED are needed to constrain effectively T_{dust} , β , (also L_{dust}) and hence get precise constraints on M_{dust} .

Constraining the **peak of the dust emission with Band 9** is crucial to obtain precise measurements of L_{dust} (which is very close to the bolometric luminosity for SMGs, and will be used to get tighter constraints on the SFR), and of the dust temperature, which will provide insight into the dust heating conditions in SMGs. A longer-wavelength **measurement in the Rayleigh-Jeans regime with Band 4** (combined with available Band 7 observations) will allow us to measure the slope of the Rayleigh-Jeans tail of the SED, which depends directly on the dust emissivity index β . This will allow us to obtain robust constraints on M_{dust} , and to understand the properties of dust at high redshift, by comparing our derived values of β with predictions from theoretical dust grain models. **Fig.4 shows that our proposed observations in Band 9, Band 7 (already in hand) and Band 4, are essential to obtain the best possible constraints of the dust mass of our galaxies (at better than 0.2 dex, i.e. at least 5 times more precise than current estimates)**, because they break the degeneracy between T_{dust} and β .

Science questions that we will address with our proposed observations:

- *Mass of dust in SMGs:* What is the dust mass distribution of our unbiased SMG sample? Can the dust masses be explained using current dust formation and growth models?
- *Properties of the dust grains:* What is the emissivity index of the dust in SMGs? What type of dust grains do we observe in the ISM of high-redshift starbursts, i.e. are the β values more consistent with carbonaceous or silicate grains? Are the dust properties the same across all SMGs, or do we see variation with galaxy properties (such as star formation activity, temperature)? Do X-ray AGN (identified and characterized in our sample by Wang et al. 2013) have any impact in the dust properties?
- *Temperature of dust in SMGs:* Is the dust hot, consistent with compact starbursts, or cooler, consistent with more extended distributions of stars and dust?
- *Gas masses derived from dust masses:* What are the gas fractions of our SMGs? What is the gas depletion timescale i.e. the SF efficiency? We will interpret the results in the context of what galaxy evolution models predict for starburst-driven mergers vs. gas-rich, secularly-evolving galaxies.

We estimate the expected total Band 9 and 4 continuum fluxes (Fig.2) using our fits to the full available UV-to-radio SED for each ALESS SMG (da Cunha et al. 2015). We propose to take snapshot observations centered at each of the brightest ALESS sources in each LESS field. Our (unresolved) continuum observations will reach a sensitivity of **1.5 mJy in Band 9 in 1.2 min, and 0.060 mJy in Band 4 in 3.3 min per snapshot (i.e. a total time on-source of 1.4 h in Band 9 and 3.8 h in Band 4 for 69 snapshots)**. This will allow us to detect the majority of our main targets (green in Fig.2) at better than 5σ level, and the faintest SMGs in the same fields as our targets (that will fall in the FOV) at $\sim 3\sigma$ confidence (grey in Fig.2).

This proposal. We propose to complete the characterization of the infrared/sub-millimeter spectral energy distributions of the ALESS SMGs by obtaining their total continuum fluxes at 679 GHz (ALMA Band 9) and at 145 GHz (ALMA Band 4). These observations will complement our current precise measurements of the total flux at 345 GHz obtained with Band 7 in Cycle 0, and will allow us to fully characterize the amount and physical properties of dust in our unbiased, well-defined sample of SMGs.

Science goal

The main goal of our proposal is **to obtain the complete dust SEDs of our unbiased and well characterized sample of SMGs**, including one flux measurement near the peak of the dust emission (with ALMA Band 9) and one flux measurement in the Rayleigh-Jeans tail of the dust emission (with Band 4).

The mass of dust in a galaxy with equilibrium temperature T_{dust} is given by $M_{\text{dust}} \propto L_{\text{dust}}/T_{\text{dust}}^{4+\beta}$, where L_{dust} is the total dust luminosity, and β is the dust emissivity index, which defines the emissivity of the dust grains as a function of frequency, and depends on the properties of the dust grains (chemical composition, size, shape). Theoretical models and laboratory studies predict a range of values for this parameter, from $\beta \simeq 1$ for small carbonaceous grains, and $\beta \simeq 2$ or higher for amorphous silicate grains (e.g. Draine & Lee 1984, Agladze et al. 1996), with some dependence on temperature. In Fig.3, we plot model dust SEDs of galaxies at $z = 2.7$ (the median redshift of our sample), with varying values of T_{dust} and β . These plots show that the shape of the dust emission is a strong function of these parameters in different wavelength ranges, and therefore observables sampling the full dust SED are needed to constrain effectively T_{dust} , β , (also L_{dust}) and hence get precise constraints on M_{dust} .

Constraining the **peak of the dust emission with Band 9** is crucial to obtain precise measurements of L_{dust} (which is very close to the bolometric luminosity for SMGs, and will be used to get tighter constraints on the SFR), and of the dust temperature, which will provide insight into the dust heating conditions in SMGs. A longer-wavelength **measurement in the Rayleigh-Jeans regime with Band 4** (combined with available Band 7 observations) will allow us to measure the slope of the Rayleigh-Jeans tail of the SED, which depends directly on the dust emissivity index β . This will allow us to obtain robust constraints on M_{dust} , and to understand the properties of dust at high redshift, by comparing our derived values of β with predictions from theoretical dust grain models. **Fig.4 shows that our proposed observations in Band 9, Band 7 (already in hand) and Band 4, are essential to obtain the best possible constraints of the dust mass of our galaxies (at better than 0.2 dex, i.e. at least 5 times more precise than current estimates)**, because they break the degeneracy between T_{dust} and β .

Science questions that we will address with our proposed observations:

- *Mass of dust in SMGs:* What is the dust mass distribution of our unbiased SMG sample? Can the dust masses be explained using current dust formation and growth models?
- *Properties of the dust grains:* What is the emissivity index of the dust in SMGs? What type of dust grains do we observe in the ISM of high-redshift starbursts, i.e. are the β values more consistent with carbonaceous or silicate grains? Are the dust properties the same across all SMGs, or do we see variation with galaxy properties (such as star formation activity, temperature)? Do X-ray AGN (identified and characterized in our sample by Wang et al. 2013) have any impact in the dust properties?
- *Temperature of dust in SMGs:* Is the dust hot, consistent with compact starbursts, or cooler, consistent with more extended distributions of stars and dust?
- *Gas masses derived from dust masses:* What are the gas fractions of our SMGs? What is the gas depletion timescale i.e. the SF efficiency? We will interpret the results in the context of what galaxy evolution models predict for starburst-driven mergers vs. gas-rich, secularly-evolving galaxies.

We estimate the expected total Band 9 and 4 continuum fluxes (Fig.2) using our fits to the full available UV-to-radio SED for each ALESS SMG (da Cunha et al. 2015). We propose to take snapshot observations centered at each of the brightest ALESS sources in each LESS field. Our (unresolved) continuum observations will reach a sensitivity of **1.5 mJy in Band 9 in 1.2 min, and 0.060 mJy in Band 4 in 3.3 min per snapshot (i.e. a total time on-source of 1.4 h in Band 9 and 3.8 h in Band 4 for 69 snapshots)**. This will allow us to detect the majority of our main targets (green in Fig.2) at better than 5σ level, and the faintest SMGs in the same fields as our targets (that will fall in the FOV) at $\sim 3\sigma$ confidence (grey in Fig.2).

This proposal. We propose to complete the characterization of the infrared/sub-millimeter spectral energy distributions of the ALESS SMGs by obtaining their total continuum fluxes at 679 GHz (ALMA Band 9) and at 145 GHz (ALMA Band 4). These observations will complement our current precise measurements of the total flux at 345 GHz obtained with Band 7 in Cycle 0, and will allow us to fully characterize the amount and physical properties of dust in our unbiased, well-defined sample of SMGs.

Science goal

The main goal of our proposal is **to obtain the complete dust SEDs of our unbiased and well characterized sample of SMGs**, including one flux measurement near the peak of the dust emission (with ALMA Band 9) and one flux measurement in the Rayleigh-Jeans tail of the dust emission (with Band 4).

The mass of dust in a galaxy with equilibrium temperature T_{dust} is given by $M_{\text{dust}} \propto L_{\text{dust}}/T_{\text{dust}}^{4+\beta}$, where L_{dust} is the total dust luminosity, and β is the dust emissivity index, which defines the emissivity of the dust grains as a function of frequency, and depends on the properties of the dust grains (chemical composition, size, shape). Theoretical models and laboratory studies predict a range of values for this parameter, from $\beta \simeq 1$ for small carbonaceous grains, and $\beta \simeq 2$ or higher for amorphous silicate grains (e.g. Draine & Lee 1984, Agladze et al. 1996), with some dependence on temperature. In Fig.3, we plot model dust SEDs of galaxies at $z = 2.7$ (the median redshift of our sample), with varying values of T_{dust} and β . These plots show that the shape of the dust emission is a strong function of these parameters in different wavelength ranges, and therefore observables sampling the full dust SED are needed to constrain effectively T_{dust} , β , (also L_{dust}) and hence get precise constraints on M_{dust} .

Constraining the **peak of the dust emission with Band 9** is crucial to obtain precise measurements of L_{dust} (which is very close to the bolometric luminosity for SMGs, and will be used to get tighter constraints on the SFR), and of the dust temperature, which will provide insight into the dust heating conditions in SMGs. A longer-wavelength **measurement in the Rayleigh-Jeans regime with Band 4** (combined with available Band 7 observations) will allow us to measure the slope of the Rayleigh-Jeans tail of the SED, which depends directly on the dust emissivity index β . This will allow us to obtain robust constraints on M_{dust} , and to understand the properties of dust at high redshift, by comparing our derived values of β with predictions from theoretical dust grain models. **Fig.4 shows that our proposed observations in Band 9, Band 7 (already in hand) and Band 4, are essential to obtain the best possible constraints of the dust mass of our galaxies (at better than 0.2 dex, i.e. at least 5 times more precise than current estimates)**, because they break the degeneracy between T_{dust} and β .

Science questions that we will address with our proposed observations:

- *Mass of dust in SMGs:* What is the dust mass distribution of our unbiased SMG sample? Can the dust masses be explained using current dust formation and growth models?
- *Properties of the dust grains:* What is the emissivity index of the dust in SMGs? What type of dust grains do we observe in the ISM of high-redshift starbursts, i.e. are the β values more consistent with carbonaceous or silicate grains? Are the dust properties the same across all SMGs, or do we see variation with galaxy properties (such as star formation activity, temperature)? Do X-ray AGN (identified and characterized in our sample by Wang et al. 2013) have any impact in the dust properties?
- *Temperature of dust in SMGs:* Is the dust hot, consistent with compact starbursts, or cooler, consistent with more extended distributions of stars and dust?
- *Gas masses derived from dust masses:* What are the gas fractions of our SMGs? What is the gas depletion timescale i.e. the SF efficiency? We will interpret the results in the context of what galaxy evolution models predict for starburst-driven mergers vs. gas-rich, secularly-evolving galaxies.

We estimate the expected total Band 9 and 4 continuum fluxes (Fig.2) using our fits to the full available UV-to-radio SED for each ALESS SMG (da Cunha et al. 2015). We propose to take snapshot observations centered at each of the brightest ALESS sources in each LEES field. Our (unresolved) continuum observations will reach a sensitivity of **1.5 mJy in Band 9 in 1.2 min, and 0.060 mJy in Band 4 in 3.3 min per snapshot (i.e. a total time on-source of 1.4 h in Band 9 and 3.8 h in Band 4 for 69 snapshots)**. This will allow us to detect the majority of our main targets (green in Fig.2) at better than 5σ level, and the faintest SMGs in the same fields as our targets (that will fall in the FOV) at $\sim 3\sigma$ confidence (grey in Fig.2).

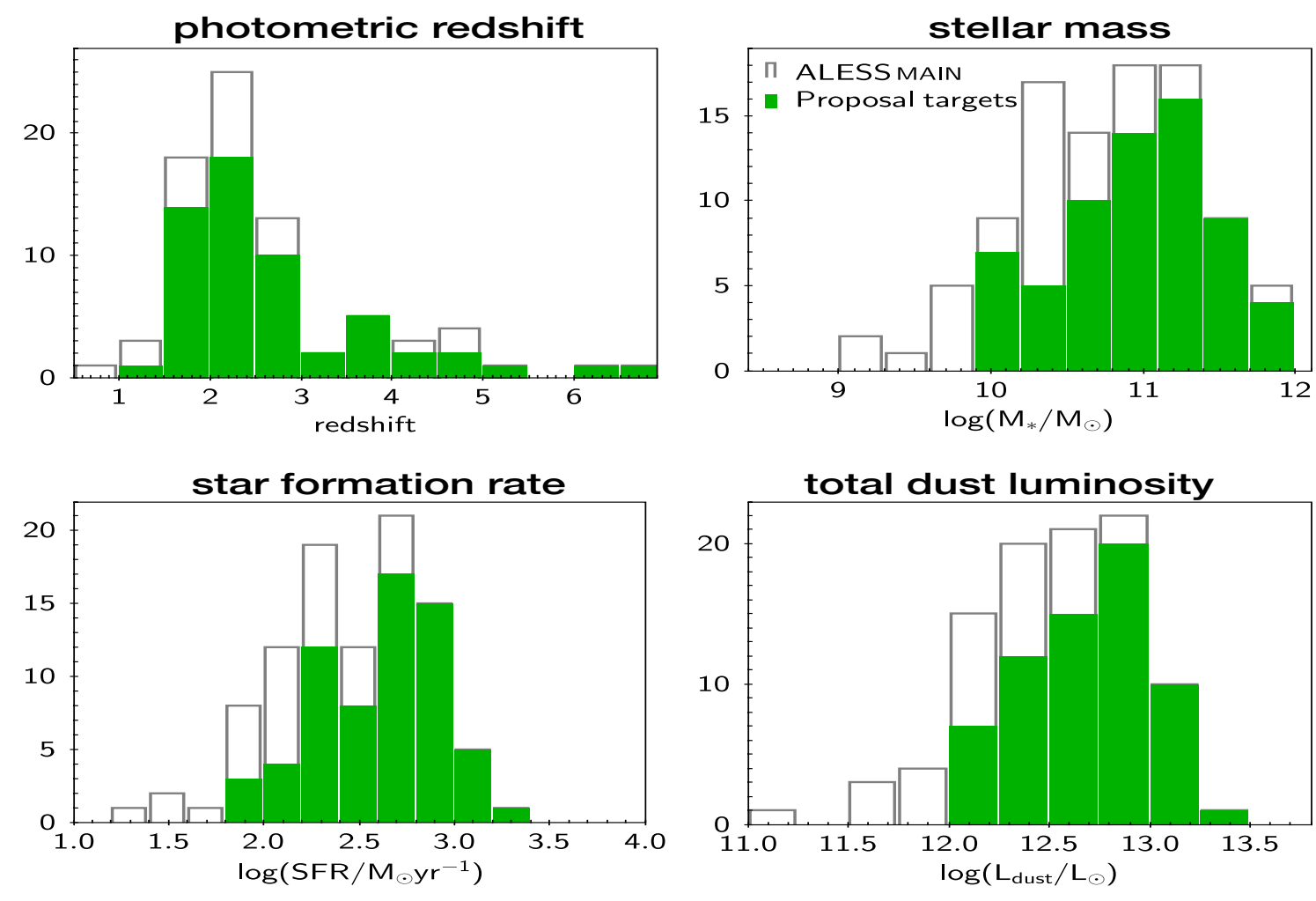


Fig. 1: Physical properties of the ALESS SMGs. Photometric redshifts derived by Simpson et al.2014; stellar masses, star formation rates and dust luminosities from da Cunha et al.2015. The median properties of the sample are: $M_* = 8.9 \times 10^{10} M_\odot$, SFR = $280 M_\odot/\text{yr}$, and $L_{\text{dust}} = 4 \times 10^{12} L_\odot$. The open grey histograms show the complete sample from the ALESS MAIN catalogue (99 SMGs); the filled green histograms show the targets of this proposal i.e. the SMGs at which our proposed continuum snapshot observations are centered: the 69 MAIN catalogue sources that are the brightest source in each LESS field. Our requested sensitivities are enough to detect even the fainter objects (grey histograms) that lie within the field-of-view of our observations centered at the targets shown in green (Fig.2).

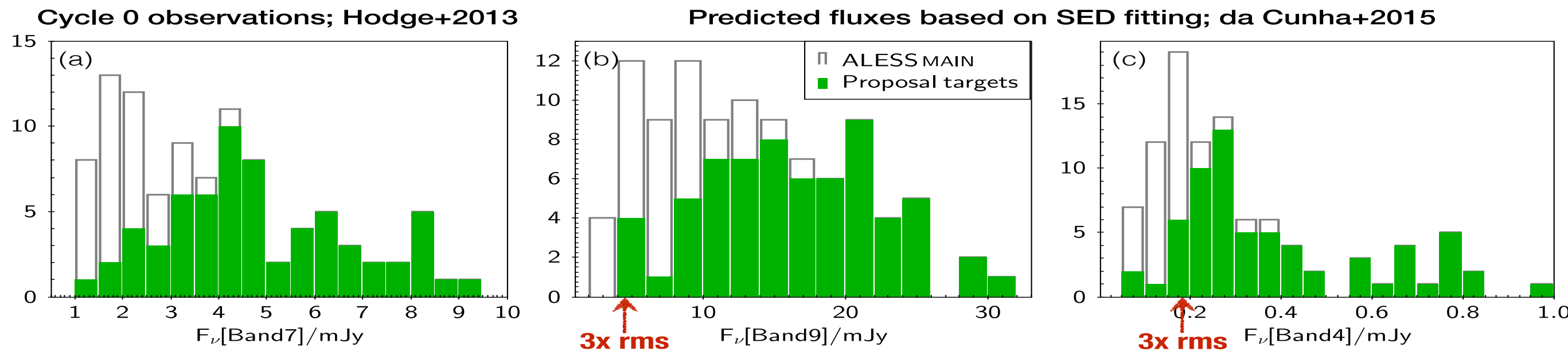


Fig. 2: (a) Distribution of the Band7 (345 GHz) continuum fluxes of the ALESS SMGs, measured from Cycle 0 observations by Hodge et al.(2013). Open grey histogram: complete sample from the ALESS MAIN catalogue; filled green histogram: the targets of this proposal: the 69 MAIN catalogue SMGs that are the brightest source in each LESS field. In panels (b) and (c), we plot the distribution of the predicted total continuum fluxes in Band 9 (679 GHz) and Band 4 (145 GHz), respectively, from SED fits to their available UV-to-radio observations using the MAGPHYS code (da Cunha et al.2008, 2015). The red arrows indicate the 3σ limit for our requested sensitivities: **1.5 mJy (i.e. 1.2 min per snapshot) in Band 9** and **60 μ Jy (i.e. 3.3 min per snapshot) in Band 4**. These sensitivities are enough to detect the majority of our main targets at better than 5σ level, and the faintest SMGs in the same fields as our targets at $\sim 3\sigma$ confidence.

Potential for publicity: This proposal is a natural follow-up to our successful Cycle 0 ALESS program (Hodge et al.2013), which warranted an ESO press release and was widely spread via social media and major news outlets. The Cycle 0 observations allowed us to build the best possible sample to study dusty starbursts in the young Universe, and our proposed Cycle 3 observations will enhance this sample by allowing the most complete physical characterization of these galaxies to date. Our data will lead to high-impact publications showcasing new science achievable with ALMA.

References

- Agladze, N. I. et al. 1996, ApJ 462, 1026 • Blain, A. W. et al. 2002, PhR 369, 111 • Casey, C. M. et al. 2014, PhR 541, 45 • da Cunha, E. et al. 2008, MNRAS 388, 1595; 2015, ApJ in press, arXiv:1504.04376 • Davé, N. et al. 2011, MNRAS 415, 11 • Dwek, E. et al. 2007, ApJ 501, 643 • Draine, B. T. & Lee, H. M. 1984, ApJ 285, 89 • Groves, B. A. et al. 2015, ApJ 799, 96 • Hayward, C. C. et al. 2011, ApJ 743, 159 • Hodge, J. A. et al. 2013, ApJ 768, 91 • Karim, A. et al. 2013, MNRAS 432, 2 • Michalowski, M. J. 2015, arXiv:1503.08210 • Morgan, H. & Edmunds 2003, MNRAS 343, 427 • Rowlands, K. et al. 2014, MNRAS 1040, 58 • Simpson, J. M. et al. 2014, ApJ 788, 125 • Scoville, N. et al. 2014, ApJ 783, 43 • Swinbank, A. M., et al. 2014, MNRAS 438, 1267 • Wang, S. X. et al. 2013, ApJ 778, 479 • Weiss, A. et al. 2009, ApJ 767, 88

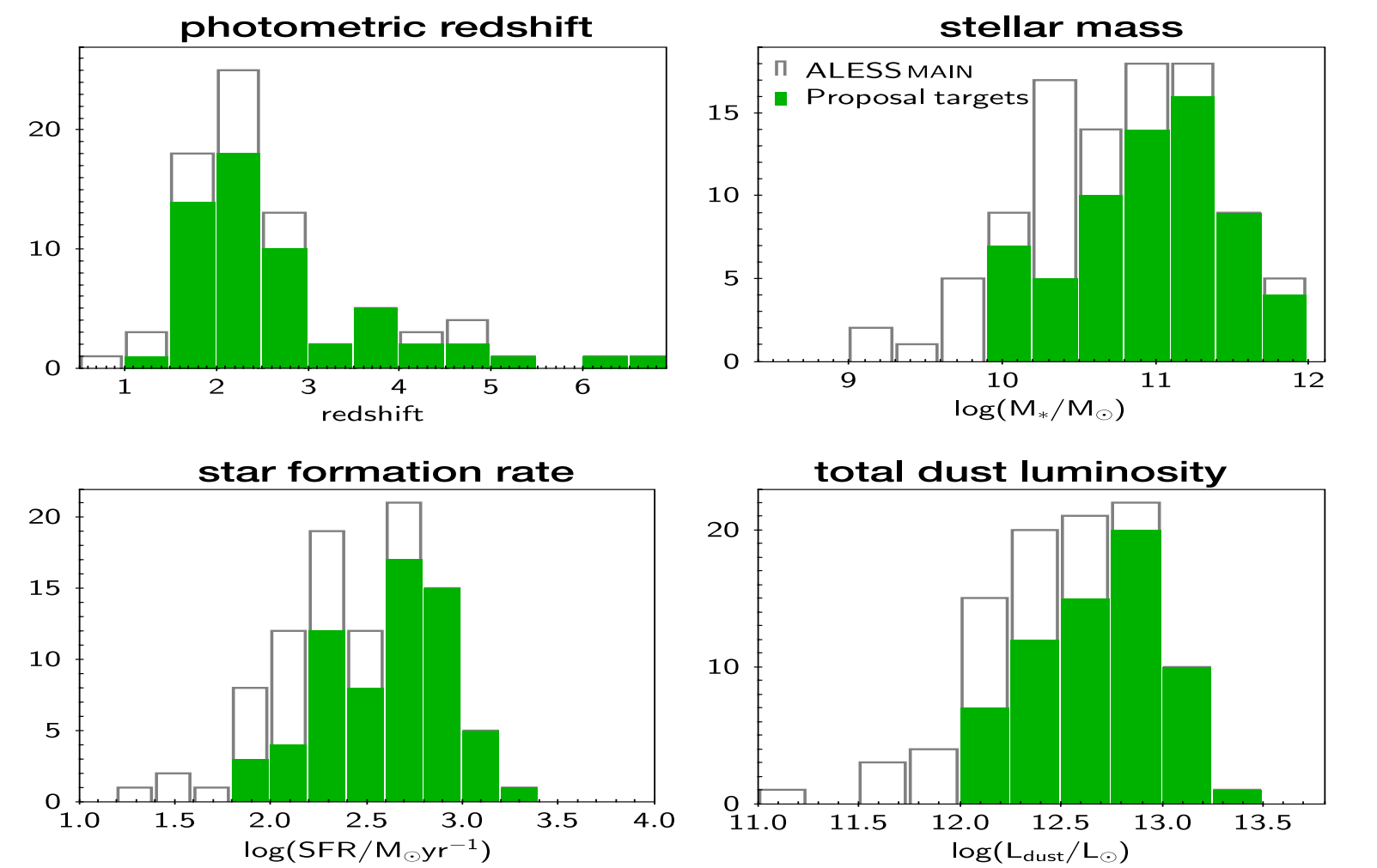


Fig. 1: Physical properties of the ALESS SMGs. Photometric redshifts derived by Simpson et al. 2014; stellar masses, star formation rates and dust luminosities from da Cunha et al. 2015. The median properties of the sample are: $M_* = 8.9 \times 10^{10} M_\odot$, SFR = $280 M_\odot/\text{yr}$, and $L_{\text{dust}} = 4 \times 10^{12} L_\odot$. The open grey histograms show the complete sample from the ALESS MAIN catalogue (99 SMGs); the filled green histograms show the targets of this proposal i.e. the SMGs at which our proposed continuum snapshot observations are centered: the 69 MAIN catalogue sources that are the brightest source in each LESS field. Our requested sensitivities are enough to detect even the fainter objects (grey histograms) that lie within the field-of-view of our observations centered at the targets shown in green (Fig. 2).

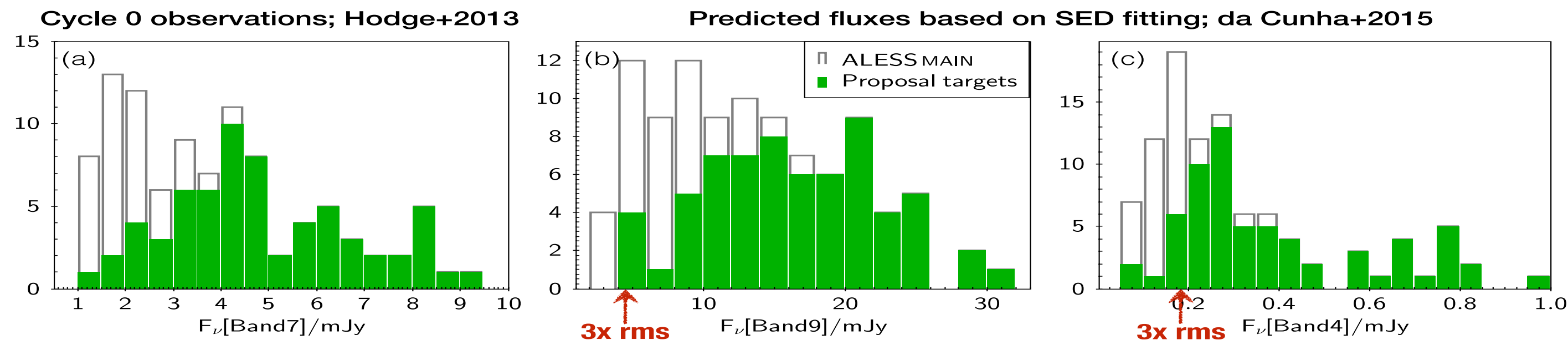


Fig. 2: (a) Distribution of the Band 7 (345 GHz) continuum fluxes of the ALESS SMGs, measured from Cycle 0 observations by Hodge et al. (2013). Open grey histogram: complete sample from the ALESS MAIN catalogue; filled green histogram: the targets of this proposal: the 69 MAIN catalogue SMGs that are the brightest source in each LESS field. In panels (b) and (c), we plot the distribution of the predicted total continuum fluxes in Band 9 (679 GHz) and Band 4 (145 GHz), respectively, from SED fits to their available UV-to-radio observations using the MAGPHYS code (da Cunha et al. 2008, 2015). The red arrows indicate the 3σ limit for our requested sensitivities: **1.5 mJy (i.e. 1.2 mJy per snapshot) in Band 9** and **60 μ Jy (i.e. 3.3 mJy per snapshot) in Band 4**. These sensitivities are enough to detect the majority of our main targets at better than 5σ level, and the faintest SMGs in the same fields as our targets at $\sim 3\sigma$ confidence.

Potential for publicity: This proposal is a natural follow-up to our successful Cycle 0 ALESS program (Hodge et al. 2013), which warranted an ESO press release and was widely spread via social media and major news outlets. The Cycle 0 observations allowed us to build the best possible sample to study dusty starbursts in the young Universe, and our proposed Cycle 3 observations will enhance this sample by allowing the most complete physical characterization of these galaxies to date. Our data will lead to high-impact publications showcasing new science achievable with ALMA.

References

- Agladze, N. I. et al. 1996, ApJ 462, 1026 • Blain, A. W. et al. 2002, PhR 369, 111 • Casey, C. M. et al. 2014, PhR 541, 45 • da Cunha, E. et al. 2008, MNRAS 388, 1595; 2015, ApJ in press, arXiv:1504.04376 • Davé, N. et al. 2011, MNRAS 415, 11 • Dwek, E. et al. 2007, ApJ 501, 643 • Draine, B. T. & Lee, H. M. 1984, ApJ 285, 89 • Groves, B. A. et al. 2015, ApJ 799, 96 • Hayward, C. C. et al. 2011, ApJ 743, 159 • Hodge, J. A. et al. 2013, ApJ 768, 91 • Karim, A. et al. 2013, MNRAS 432, 2 • Michalowski, M. J. 2015, arXiv:1503.08210 • Morgan, H. & Edmunds 2003, MNRAS 343, 427 • Rowlands, K. et al. 2014, MNRAS 1040, 58 • Simpson, J. M. et al. 2014, ApJ 788, 125 • Scoville, N. et al. 2014, ApJ 783, 43 • Swinbank, A. M., et al. 2014, MNRAS 438, 1267 • Wang, S. X. et al. 2013, ApJ 778, 479 • Weiss, A. et al. 2009, ApJ 767, 88

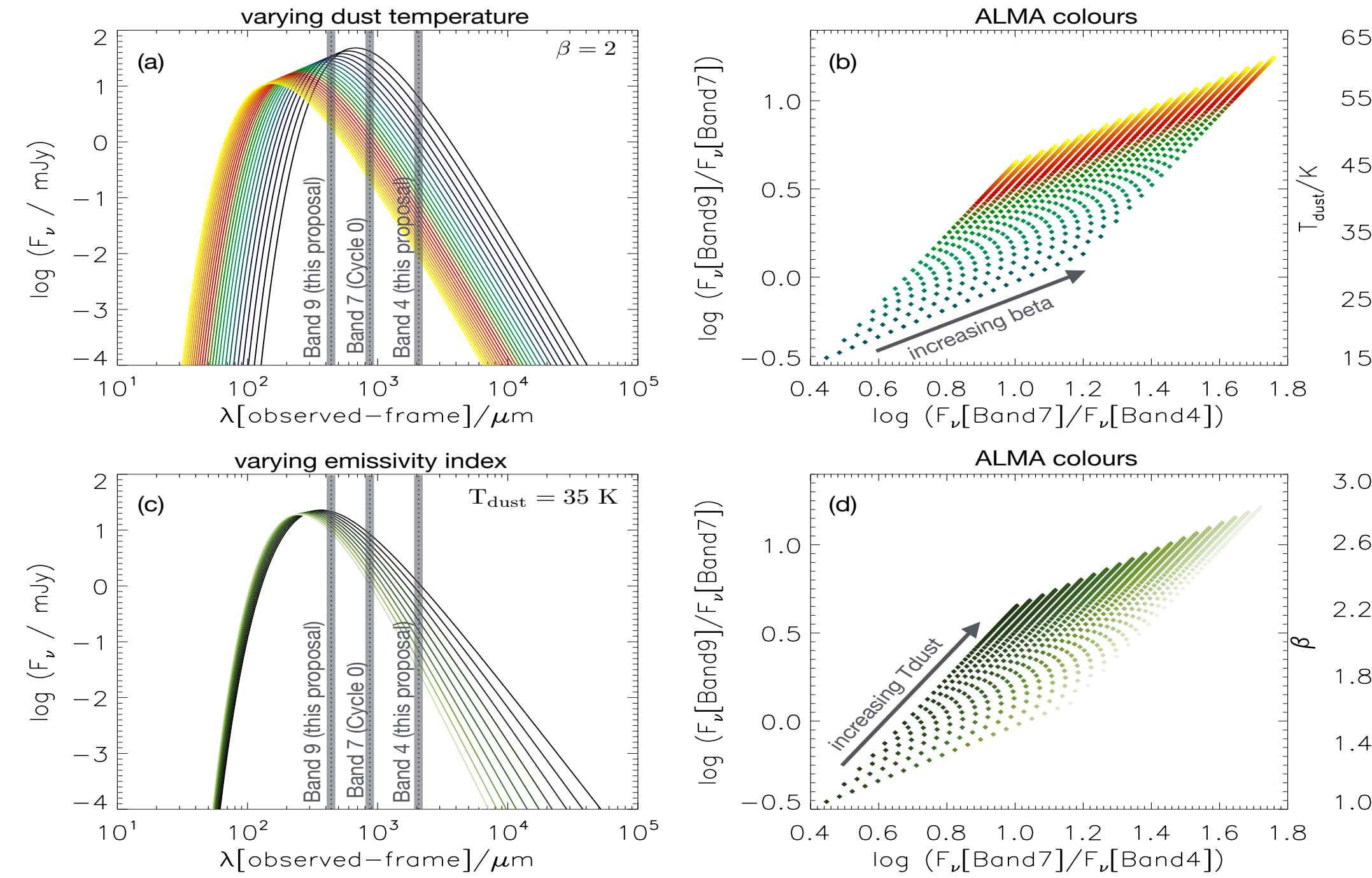


Fig. 3: The combination of Band 7 observations from Cycle 0 and the two continuum measurements requested in this proposal in Band 9 and Band 4 are crucial to constrain the dust mass, because they break the degeneracy between the dust temperature and the emissivity index. Panels (a) and (c) show the variation of dust emission at $z = 2.7$ (the median redshift of our sample) with dust temperature T_{dust} at fixed emissivity index β (and vice-versa). Panels (b) and (d) show how the ALMA colours in the three bands (Band9/Band7 and Band7/Band4) vary for a grid of models with varying T_{dust} and β . These plots show that these two crucial parameters are orthogonal in our chosen colour space, and therefore by adding Bands 9 and 4 to our existing Band 7 data we can optimally constrain the dust temperature and emissivity simultaneously, therefore obtaining the most robust estimates of the dust mass to date. We note that, for simplicity, we focus on the cold dust in galaxies, which largely dominates the total dust mass. Our SED modelling includes several dust temperature components (da Cunha et al. 2008, 2015), but the importance of our proposed observations on constraining the dust mass holds in the context of our multi-component models.

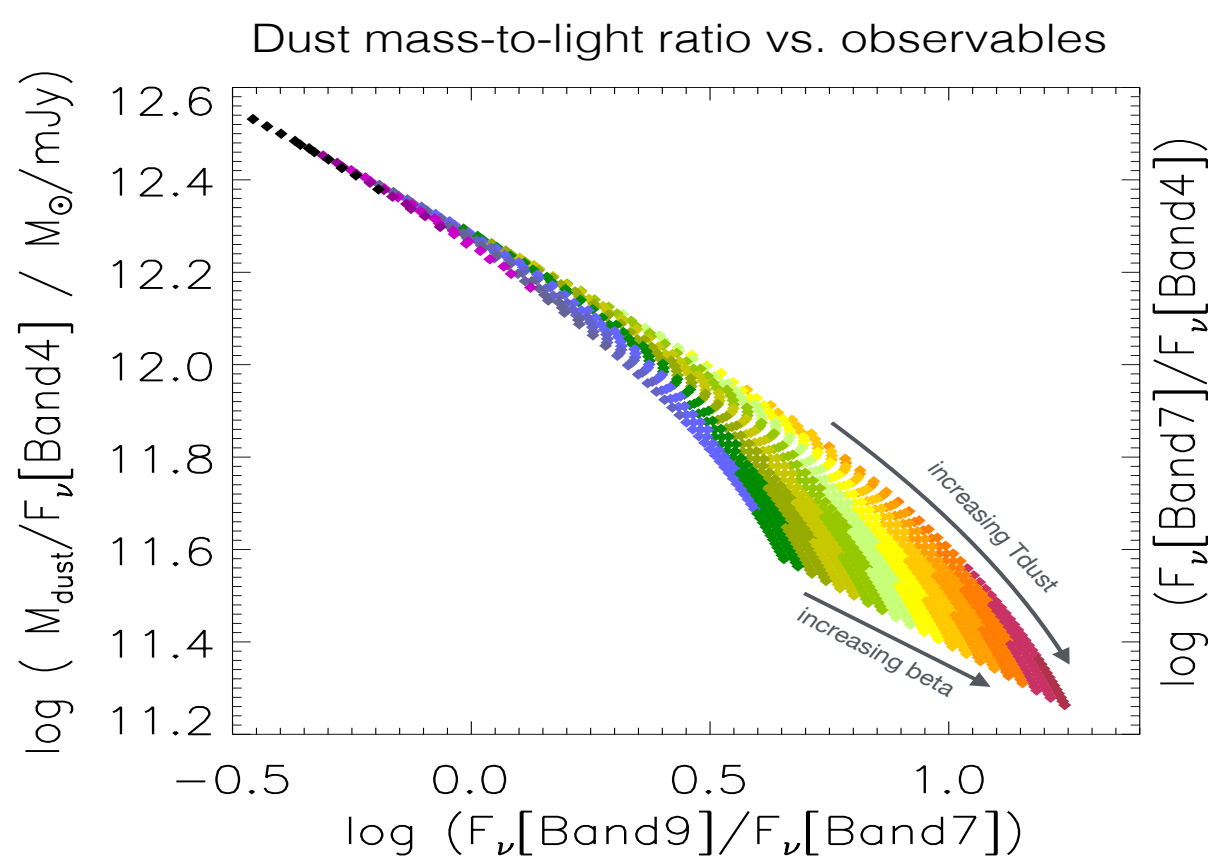


Fig. 4: Our proposed observations are crucial to constrain the dust mass, as can be seen for the dependence of the dust mass per unit flux in Band 4 on the Band9/Band7 and Band7/Band4 colours, for a range of dust temperatures and emissivity indexes (Fig.3). At fixed Band7/Band4 colour (which constrains β), the dust mass-to-light ratio is a tight function of Band9/Band7 colour (which constrains T_{dust}). **Our requested Band 4 and Band 9 flux measurements at $S/N \simeq 5$ and better, combined with Band 7 fluxes already in hand, will allow us to constrain the dust masses of our SMGs to within 0.2 dex or better, i.e. 5 times more precisely than our current estimates (da Cunha et al. 2015), and will allow us to constrain the emissivity index (which tells us about dust grain properties) for the first time for these galaxies.**

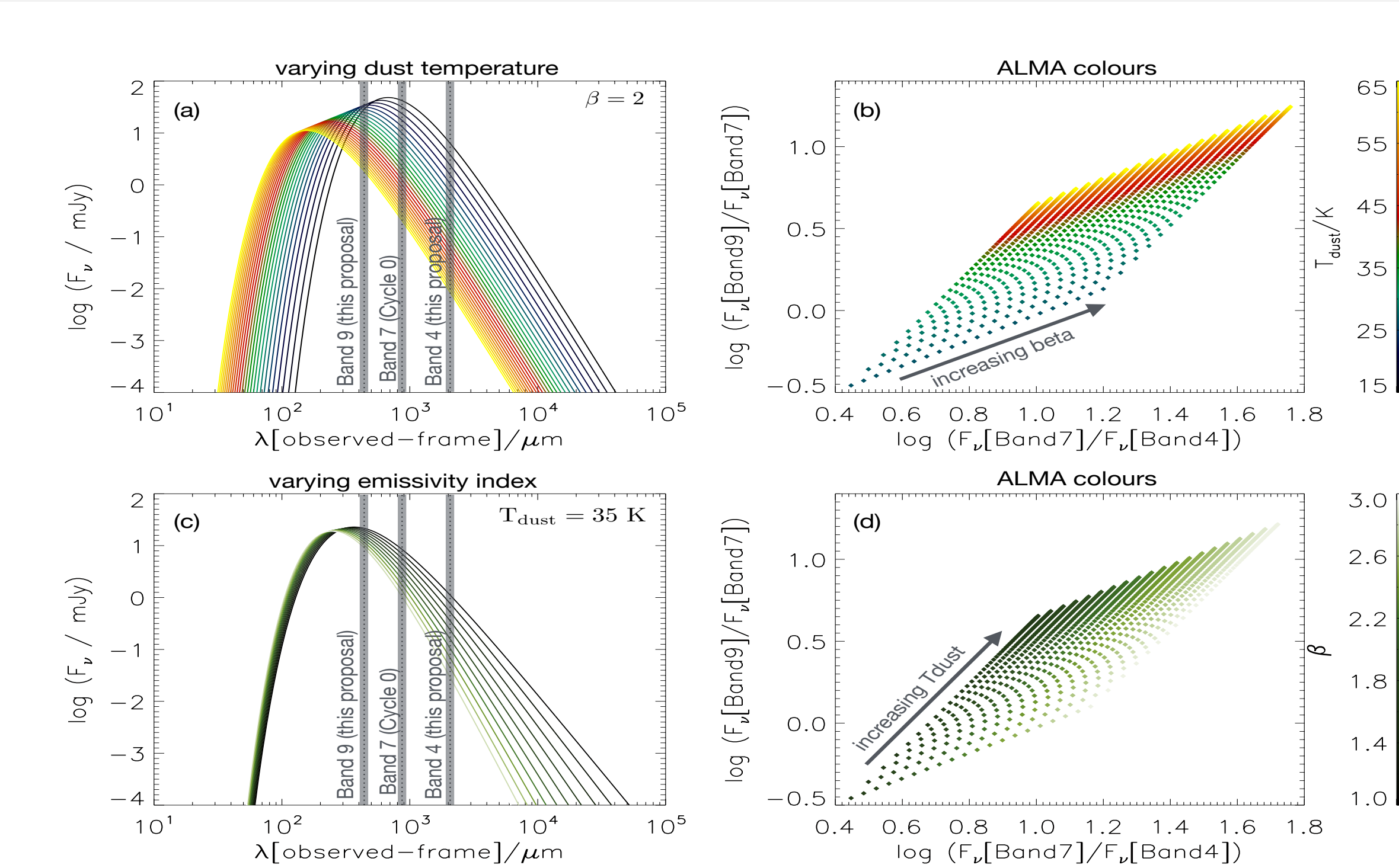


Fig. 3: The combination of Band 7 observations from Cycle 0 and the two continuum measurements requested in this proposal in Band 9 and Band 4 are crucial to constrain the dust mass, because they break the degeneracy between the dust temperature and the emissivity index. Panels (a) and (c) show the variation of dust emission at $z = 2.7$ (the median redshift of our sample) with dust temperature T_{dust} at fixed emissivity index β (and vice-versa). Panels (b) and (d) show how the ALMA colours in the three bands (Band9/Band7 and Band7/Band4) vary for a grid of models with varying T_{dust} and β . These plots show that these two crucial parameters are orthogonal in our chosen colour space, and therefore by adding Bands 9 and 4 to our existing Band 7 data we can optimally constrain the dust temperature and emissivity simultaneously, therefore obtaining the most robust estimates of the dust mass to date. We note that, for simplicity, we focus on the cold dust in galaxies, which largely dominates the total dust mass. Our SED modelling includes several dust temperature components (da Cunha et al. 2008, 2015), but the importance of our proposed observations on constraining the dust mass holds in the context of our multi-component models.

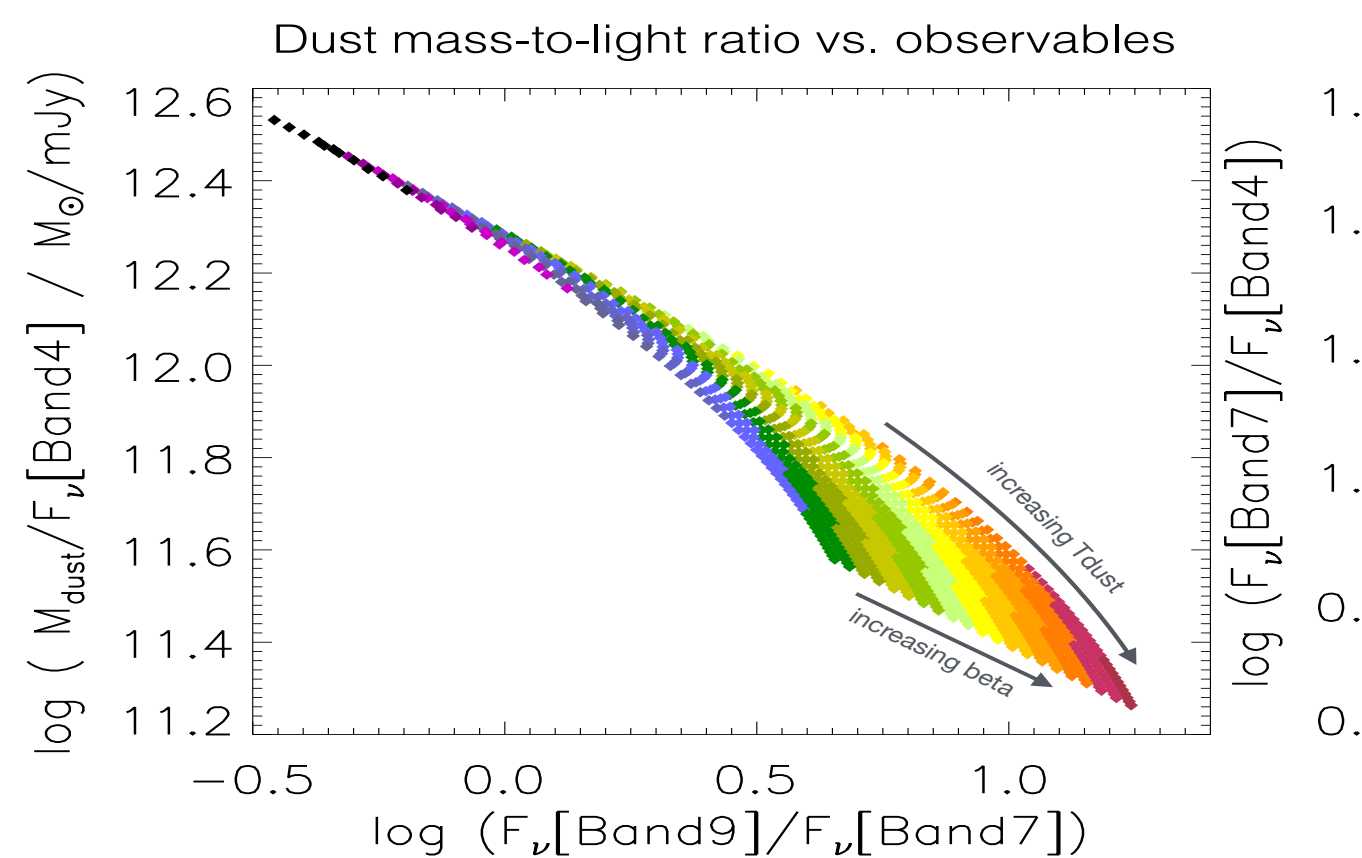


Fig. 4: Our proposed observations are crucial to constrain the dust mass, as can be seen for the dependence of the dust mass per unit flux in Band 4 on the Band9/Band7 and Band7/Band4 colours, for a range of dust temperatures and emissivity indexes (Fig.3). At fixed Band7/Band4 colour (which constrains β), the dust mass-to-light ratio is a tight function of Band9/Band7 colour (which constrains T_{dust}). **Our requested Band 4 and Band 9 flux measurements at $S/N \simeq 5$ and better, combined with Band 7 fluxes already in hand, will allow us to constrain the dust masses of our SMGs to within 0.2 dex or better, i.e. 5 times more precisely than our current estimates (da Cunha et al. 2015), and will allow us to constrain the emissivity index (which tells us about dust grain properties) for the first time for these galaxies.**

Technical Justification

2015.1.00948.S

SG : 1 of 2 Band 4 continuum snapshots Band 4

Band 4 continuum imaging of the ALESS SMGs.

Science Goal Parameters

Ang.Res.	LAS	Requested RMS	RMS Bandwidth	Rep.Freq.	Cont. RMS	Cont. Bandwidth	Poln.Prod.	Non-standard mode
2.30"	1.0"	60 μJy, 600.2 μK	14792.391 km/s, 7.5 GHz	152.000000 GHz	59.87 μJy, 599 μK	7.500 GHz	XX,YY	No

Use of 12m Array (36 antennas)

t_total (all configs)	t_science (extended)	t_total(compact)	Imaged area	#12m pointing	12m Mosaic spacing	HPBW	t_per_point	Data Vol	Data Rate
6.3 h	3.8 h	0.0 s	12.8 "	69	offset	38.3 "	201.1 s	54.2 GB	2.4 MB/s

Use of ACA 7m Array (10 antennas) and TP Array

t_total(ACA)	t_total(7m)	t_total(TP)	Imaged area	#7m pointing	7m Mosaic spacing	HPBW	t_per_point	Data Vol	Data Rate

69 Targets

No	Target	Ra,Dec(J2000)	V,def,frame --OR--z
1	1-ALESS001.1	03:33:14, -27:56:14	0.00 km/s, lsrk, RADIO
2	2-ALESS002.1	03:33:02, -27:56:42	0.00 km/s, lsrk, RADIO
3	3-ALESS003.1	03:33:21, -27:55:20	0.00 km/s, lsrk, RADIO
4	4-ALESS005.1	03:31:28, -27:59:09	0.00 km/s, lsrk, RADIO
5	5-ALESS006.1	03:32:56, -28:01:00	0.00 km/s, lsrk, RADIO
6	6-ALESS007.1	03:33:15, -27:45:24	0.00 km/s, lsrk, RADIO
7	7-ALESS009.1	03:32:11, -27:52:11	0.00 km/s, lsrk, RADIO
8	8-ALESS010.1	03:32:19, -27:52:14	0.00 km/s, lsrk, RADIO
9	9-ALESS011.1	03:32:13, -27:56:00	0.00 km/s, lsrk, RADIO
10	10-ALESS013.1	03:32:48, -27:42:51	0.00 km/s, lsrk, RADIO
11	11-ALESS014.1	03:31:52, -28:03:19	0.00 km/s, lsrk, RADIO
12	12-ALESS015.1	03:33:33, -27:59:29	0.00 km/s, lsrk, RADIO
13	13-ALESS017.1	03:32:07, -27:51:20	0.00 km/s, lsrk, RADIO
14	14-ALESS018.1	03:32:04, -27:46:47	0.00 km/s, lsrk, RADIO
15	15-ALESS019.1	03:32:08, -27:58:14	0.00 km/s, lsrk, RADIO
16	16-ALESS022.1	03:31:46, -27:32:39	0.00 km/s, lsrk, RADIO
17	17-ALESS023.1	03:32:12, -28:05:06	0.00 km/s, lsrk, RADIO
18	18-ALESS025.1	03:31:56, -27:59:39	0.00 km/s, lsrk, RADIO
19	19-ALESS029.1	03:33:36, -27:58:09	0.00 km/s, lsrk, RADIO
20	20-ALESS031.1	03:31:49, -27:57:40	0.00 km/s, lsrk, RADIO
21	21-ALESS035.1	03:31:10, -27:37:15	0.00 km/s, lsrk, RADIO
22	22-ALESS037.1	03:33:36, -27:53:50	0.00 km/s, lsrk, RADIO
23	23-ALESS039.1	03:31:45, -27:34:36	0.00 km/s, lsrk, RADIO
24	24-ALESS041.1	03:31:10, -27:52:36	0.00 km/s, lsrk, RADIO
25	25-ALESS043.1	03:33:06, -27:48:02	0.00 km/s, lsrk, RADIO
26	26-ALESS045.1	03:32:25, -27:52:30	0.00 km/s, lsrk, RADIO
27	27-ALESS049.1	03:31:24, -27:50:47	0.00 km/s, lsrk, RADIO
28	28-ALESS051.1	03:31:45, -27:44:27	0.00 km/s, lsrk, RADIO
29	29-ALESS055.1	03:33:02, -27:40:35	0.00 km/s, lsrk, RADIO
30	30-ALESS057.1	03:31:51, -27:53:27	0.00 km/s, lsrk, RADIO
31	31-ALESS059.2	03:33:03, -27:44:18	0.00 km/s, lsrk, RADIO
32	32-ALESS061.1	03:32:45, -28:00:23	0.00 km/s, lsrk, RADIO
33	33-ALESS063.1	03:33:08, -28:00:43	0.00 km/s, lsrk, RADIO
34	34-ALESS065.1	03:32:52, -27:35:20	0.00 km/s, lsrk, RADIO
35	35-ALESS066.1	03:33:31, -27:54:09	0.00 km/s, lsrk, RADIO
36	36-ALESS067.1	03:32:43, -27:55:14	0.00 km/s, lsrk, RADIO
37	37-ALESS068.1	03:32:33, -27:39:13	0.00 km/s, lsrk, RADIO
38	38-ALESS069.1	03:31:33, -27:59:32	0.00 km/s, lsrk, RADIO
39	39-ALESS070.1	03:31:44, -27:38:35	0.00 km/s, lsrk, RADIO
40	40-ALESS071.1	03:33:05, -27:33:28	0.00 km/s, lsrk, RADIO
41	41-ALESS072.1	03:32:40, -27:37:58	0.00 km/s, lsrk, RADIO
42	42-ALESS073.1	03:32:29, -27:56:19	0.00 km/s, lsrk, RADIO
43	43-ALESS074.1	03:33:09, -27:48:17	0.00 km/s, lsrk, RADIO
44	44-ALESS075.1	03:31:27, -27:55:51	0.00 km/s, lsrk, RADIO
45	45-ALESS076.1	03:33:32, -27:59:55	0.00 km/s, lsrk, RADIO
46	46-ALESS079.1	03:32:21, -27:56:26	0.00 km/s, lsrk, RADIO
47	47-ALESS080.1	03:31:42, -27:48:36	0.00 km/s, lsrk, RADIO
48	48-ALESS082.1	03:32:54, -27:38:14	0.00 km/s, lsrk, RADIO
49	49-ALESS083.4	03:33:08, -28:05:18	0.00 km/s, lsrk, RADIO
50	50-ALESS084.1	03:31:54, -27:51:05	0.00 km/s, lsrk, RADIO
51	51-ALESS087.1	03:32:50, -27:31:41	0.00 km/s, lsrk, RADIO
52	52-ALESS088.1	03:31:54, -27:53:41	0.00 km/s, lsrk, RADIO
53	53-ALESS092.2	03:31:38, -27:43:43	0.00 km/s, lsrk, RADIO
54	54-ALESS094.1	03:33:07, -27:58:05	0.00 km/s, lsrk, RADIO
55	55-ALESS098.1	03:31:29, -27:57:22	0.00 km/s, lsrk, RADIO
56	56-ALESS099.1	03:32:51, -27:55:33	0.00 km/s, lsrk, RADIO
57	57-ALESS102.1	03:33:35, -27:40:23	0.00 km/s, lsrk, RADIO
58	58-ALESS103.3	03:33:25, -27:34:01	0.00 km/s, lsrk, RADIO
59	59-ALESS107.1	03:31:30, -27:51:49	0.00 km/s, lsrk, RADIO
60	60-ALESS110.1	03:31:22, -27:54:17	0.00 km/s, lsrk, RADIO
61	61-ALESS112.1	03:32:48, -27:31:13	0.00 km/s, lsrk, RADIO
62	62-ALESS114.1	03:31:50, -27:44:45	0.00 km/s, lsrk, RADIO
63	63-ALESS115.1	03:33:49, -27:42:34	0.00 km/s, lsrk, RADIO
64	64-ALESS116.1	03:31:54, -27:45:28	0.00 km/s, lsrk, RADIO
65	65-ALESS118.1	03:31:21, -27:49:41	0.00 km/s, lsrk, RADIO
66	66-ALESS119.1	03:32:56, -28:03:25	0.00 km/s, lsrk, RADIO
67	67-ALESS122.1	03:31:39, -27:41:19	0.00 km/s, lsrk, RADIO
68	68-ALESS124.1	03:32:04, -27:36:06	0.00 km/s, lsrk, RADIO
69	69-ALESS126.1	03:32:09, -27:41:07	0.00 km/s, lsrk, RADIO

Expected Source Properties

	Peak Flux	SNR	Pol.	Pol. SNR	Linewidth	RMS (over 1/3 linewidth)	linewidth / bandwidth used for sensitivity
Line	0.00 μJy	0.0	0.0%	0.0	0 km/s		
Continuum	89.92 μJy	1.5	0.0%	0.0	0 km/s		

Dynamic range (cont flux/line rms): N/A

Spectral Setup : Single Continuum

Center Freq (Sky)	Center Freqs. SPWs	Eff #Ch p.p.	Bandwidth	Resolution	Vel. Bandwidth	Vel. Resolution	RMS
145.000000	138.000000	128	1875.00 MHz	15.625 MHz	4073.3 km/s	67.888 km/s	114.89 μJy, 1.4 mK
	140.000000	128	1875.00 MHz	15.625 MHz	4015.1 km/s	66.918 km/s	115.22 μJy, 1.4 mK
	150.000000	128	1875.00 MHz	15.625 MHz	3747.4 km/s	62.457 km/s	118.86 μJy, 1.2 mK
	152.000000	128	1875.00 MHz	15.625 MHz	3698.1 km/s	61.635 km/s	120 μJy, 1.2 mK

Justification for requested RMS and resulting S/N (and for spectral lines the bandwidth selected) for the sensitivity calculation.

Band choice: we request continuum observations at 145GHz (Band 4), in order to sample the Rayleigh-Jeans tail of the dust emission in our SMGs.

Bandwidth: 7.5GHz, i.e. the total bandwidth for continuum observations.

Requested sensitivity: we estimate the continuum fluxes in Band 4 for each of our targets using their multi-wavelength spectral energy distribution fits presented in da Cunha et al. 2015. These predictions are essentially extrapolations of their dust emission SEDs which are consistent with available observations for each target in the UV, optical, infrared and radio. The distribution of predicted target fluxes in Band 4 is plotted in Fig.2(c).

Since we are requesting unresolved observations, we set the predicted continuum flux density of each target to be equal to the total flux density.

Our requested RMS of 60 uJy/beam is necessary to get at least 3sigma detections for the vast majority of our main targets (plotted in green in Fig.2).

For most targets, the S/N will be much higher, as shown in Fig.2(c), which is needed for our program.

The chosen setup will result in high S/N detections in the majority of targets. Removing the very few faint sources from the sample does not really save observing time, which is why we decided to cover all ALESS sources to uniform depth.

Justification of the chosen angular resolution and largest angular scale for the source(s) in this Science Goal.

From our Cycle 0 Band 7 imaging program at 1.6arcsec resolution, we find that the vast majority of our targets are unresolved or marginally resolved, with deconvolved sizes \sim 1 arcsec (Hodge et al. 2013).

Therefore, we set the largest angular scale to 1 arcsec, which means we do not need ACA observations.

We request an angular resolution of 2.3 arcsec in Band 4 (achievable with the most compact antenna configuration in Cycle 3, C36-1) which, based on the Band 7 Cycle 0 observations, is sufficient to separate the different sources in fields where there are multiple ALESS SMGs and, because the SMGs will be unresolved at this resolution, will allow us to measure the total fluxes. Better angular resolutions achieved with more extended antenna configurations, 1.2 arcsec with configuration C36-2 and 0.8 arcsec with configuration C36-3 would also be acceptable.

Justification of the correlator set-up with particular reference to the number of spectral resolution elements per line width.

We request only continuum observations using the OT standard optimized frequencies for Band 4.

Assignment 2 (due May 25th)

Collaborative
assignment:
3 groups of 3 people

Write a title, abstract and scientific justification for an observing or supercomputing proposal.

Abstract <100 words.

The whole document should be **2 pages at most**, including references (11pt or larger font).

The **scientific justification** needs to include:

- an introduction to the problem (this should be brief/to the point; there should be *no more* than 2-3 key science questions);
- how you will solve the problem (this should include a brief survey design for a telescope proposal/an outline of the simulations you would run for a supercomputing proposal; you can talk to supervisors/seek advice from experts on this);
- a description of what would be innovative about these observations/simulations;
- a justification of resources (why is it essential to use this facility?): this should include a statement on the feasibility of your study;
- at least one figure/table, ideally two (this can be hand-drawn);
- good use of formatting.

Assignment 2 (due May 25th)

Collaborative
assignment:
3 groups of 3 people

Total marks available: 100

Grading
Scheme

Content Marks (Total marks available for content: 80)



Content	Mark	Comments
Clear, persuasive abstract/project summary. Less than 100 words.	/20	
Introduction to the problem (2 -3 key science questions) and how you will solve it.	/20	
A description of what is innovative about the proposal.	/10	
A justification of the resources.	/10	
Inclusion of relevant figures.	/10	
Good use of persuasive language (targeted at audience, not too much jargon).	/10	

Assignment 2 (due May 25th)

Collaborative
assignment:
3 groups of 3 people

Formatting Marks (Total marks available for content: 20)

Grading
Scheme

Formatting	Mark	Comments
Less than 2 pages	/5	
Clear figure	/5	
Use of headings/formatting to highlight key points.	/10	

Assignment 2 (due May 25th)

- Measure the redshift of a galaxy (or galaxy sample).
- Obtain a high-resolution image of the stellar emission of a galaxy (or sample).
- Measure the kinematics/rotation curve of a galaxy using IFU.
- Measure the CO line of a galaxy (to get molecular mass).
- Measure the age of a cluster via an H-R diagram.
- Detect the transit of an exoplanet, in one wavelength band or several.
- Measure the metallicity of a galaxy (or sample).
- Detect the Lyman forest towards a distant QSO.
- Run a simulation investigating the effect of stellar feedback on galaxies.